UNIVERSIDADE FEDERAL DE SANTA CATARINA
CAMPUS UNIVERSITÁRIO - TRINDADE
PROGRAMA DE PÓS-GRADUAÇÃO EM ENGENHARIA QUÍMICA

Mariana Schneider

Stability and efficiency of silica-based nanofluids for enhanced oil recovery

Florianópolis

2022

Mariana Schneider

Stability and efficiency of silica-based nanofluids for enhanced oil recovery

Florianópolis

2022

Mariana Schneider

Stability and efficiency of silica-based nanofluids for enhanced oil recovery

The present work at the master level was evaluated and approved by an examining board composed of the following members:

Prof. Bruno Francisco Oechsler, Dr.
Universidade Federal de Santa Catarina – UFSC

Prof. Maria José Jerônimo de Santana Ponte, Dr.
Universidade Federal do Paraná

Prof. Suelen Maria de Amorim, Dr.
Universidade Federal do Sul e Sudeste do Pará

We certify that this is the **original and final version** of the dissertation that was considered appropriate to obtain the Title of MSc in the Chemical Engineering Graduate Program.

_____

Prof. Débora de Oliveira, Dr.
Program Coordinator

_____

Prof. Regina de Fátima Peralta Muniz Moreira Dr.
Advisor

Florianópolis, May 2022.

I dedicate this work to my parents and friends
who helped me along the way.

ACKNOWLEDGMENTS

You've got to find what you love. And that is as true for your work as it is for your lovers. Your work is going to fill a large part of your life, and the only way to be truly satisfied is to do what you believe is great work. And the only way to do great work is to love what you do.

(STEVE JOBS, 2005)

RESUMO

O uso de nanofluidos em recuperação avançada de petróleo tem ganhado atenção devido à possibilidade de intensificar a recuperação de petróleo de campos de petróleo maduros. Diferentes mecanismos são envolvidos quando nanofluidos são injetados em reservatórios de petróleo, como alteração da molhabilidade, redução da tensão interfacial, aumento da viscosidade da solução aquosa e diminuição da viscosidade do óleo. As nanopartículas de sílica são amplamente utilizadas para formulações de nanofluidos, mas existem obstáculos importantes para o uso de nanofluidos na recuperação avançada de petróleo. A estabilidade é o mais evidente, além dos aspectos ambientais e econômicos, e a necessidade de projetar processos de produção em larga escala adequados para a síntese de nanopartículas com as características exigidas. Assim, este estudo tem como objetivo avaliar a estabilidade e eficiência do uso de diferentes fontes de nanopartículas de sílica na formulação de nanofluidos aplicáveis à recuperação avançada de petróleo. Foram utilizadas nanopartículas de sílica sintetizadas a partir de cinzas de casca de arroz, nanopartículas precipitada por meio do método sol-gel, e uma amostra comercial de nanopartículas de sílica. O efeito das características das nanopartículas, tais como forma, tamanho, concentração, características hidrofílicas/hidrofóbicas e suas interações com surfactante e óleo, é discutido em termos da taxa de recuperação de óleo. As nanopartículas de sílica foram caracterizadas por FRX, DRX, MEV, MET, FTIR, XPS e área superficial específica. Os nanofluidos com diferentes concentrações de nanopartículas foram caracterizados em termos de sua viscosidade, tensão superficial, potencial zeta e estabilidade. A recuperação de óleo aumentou devido à injeção de nanofluido após a recuperação secundária. Uma recuperação de óleo adicional de 5-10% foi alcançada após a inundação com nanofluidos, provando que a sílica da cinza da casca de arroz tem eficiência comparável a outras nanopartículas de sílica sintética para serem usadas na recuperação avançada de petróleo.

Palavras-Chave: Nanofluidos, Nanopartículas, Sílica, Síntese, Recuperação Avançada de Petróleo.

RESUMO EXPANDIDO

Introdução

A nanotecnologia é a área da ciência dedicada a entender os fundamentos da física, química, biologia e tecnologia de materiais em nanoescala (Ali et al., 2018). Devido a essa característica, a nanotecnologia tem aplicações em diversas áreas do conhecimento, como engenharia, química, física, biologia, medicina, entre outras. As nanopartículas (NP) podem ser dispersas em bases fluidas, como etilenoglicol, óleo, água, salmoura, surfactantes etc., para preparar nanofluidos (Maaref et al., 2020; Hou et al., 2022; Sircar et al., 2022). Dependendo das características da nanopartícula a estabilidade e as propriedades térmicas, ópticas, elétricas, reológicas e magnéticas podem ser ajustadas para diferentes aplicações (Awais et al., 2021; Suleimanov et al., 2011). Na indústria do petróleo, as nanopartículas têm sido aplicadas em operações de perfuração, tratamento de águas residuais, inibição de corrosão, desenvolvimento de produção, transferência de calor e recuperação avançada de petróleo (Ali et al., 2020; Ali et al., 2020a; Abang et al., 2021; Mittal, 2022). A recuperação de petróleo ocorre em três etapas: recuperação primária, secundária e terciária. Na recuperação primária, a energia natural presente no reservatório é utilizada, e apenas cerca de 5-10% do óleo presente no reservatório é recuperado. Na recuperação secundária, água e/ou gás são injetados no reservatório, e a recuperação de óleo é de 10-55% em média. Sendo assim, após a recuperação primária e secundária, uma grande quantidade de óleo permanece nos poros do reservatório, devido à alta pressão capilar da água. Desta forma, para aumentar o fator de recuperação, diversos métodos, como biológicos, físicos e químicos podem ser aplicados, na recuperação terciária, também conhecida como recuperação avançada de petróleo (EOR). Dentro do método químico, está a utilização de nanofluidos, que permite que um adicional de 5-15% do óleo do reservatório seja recuperado (Viswanathan, 2016). Nesse método, a associação entre nanopartículas e surfactantes para preparar nanofluidos para aplicações em EOR tem sido proposta por vários autores nos últimos anos (Agi et al., 2020; Ali et al., 2020; Ali et al., 2020a; Schneider et al., 2021; Lau et al., 2017; Behera et al., 2022; Mittal, 2022; Sircar et al., 2022). Embora as nanopartículas mais utilizadas sejam as de dióxido de silício, estudos relataram o uso de diversas nanopartículas como dióxido de titânio, óxido de grafeno, óxido de alumínio, óxido de Ferro, entre outras. Visto isso, o método de preparação de nanopartículas pode desempenhar um papel fundamental no controle de suas propriedades físico-químicas, como tamanho, morfologia e ponto de carga zero, influenciando na estabilidade do nanofluido (Said et al., 2021). Alguns exemplos de métodos de preparação amplamente aceitos para a síntese de nanopartículas são hidrotérmico (Raj et al., 2019), co-precipitação (Shalbafan et al., 2019), sol-gel (Negi et al., 2021), deposição de vapor químico (Awais et al., 2018) e biossíntese (Zamani et al., 2021). Outros métodos menos comuns também são aplicados, como a moagem (Agi et al., 2020), e o processo Stöber (Wang et al., 2010). No entanto, estudos mais profundos são necessários para formular nanofluidos para evitar a aglomeração de nanopartículas e aumentar a recuperação de óleo ajustando as condições operacionais, como a concentração das nanopartículas e a composição do nanofluido. Por fim, este estudo tem como objetivo comparar a eficiência da sílica produzida a partir de cinza de casca de arroz, sílica comercial e sílica precipitada utilizando o método sol-gel no processo de recuperação avançada de óleo.

Objetivos

O principal objetivo deste estudo é preparar e caracterizar nanopartículas e nanofluidos à base de sílica e avaliar o efeito de nanofluidos à base de sílica na recuperação avançada de petróleo. Além disso, para atingir o objetivo principal, são propostos os seguintes objetivos específicos: (i) Determinar a composição química e a química da superfície das nanopartículas; (ii) Analisar a estrutura (morfologia, estrutura cristalina e microestruturas), área de superfície e distribuição do tamanho dos poros das nanopartículas; (iii) Determinar o comportamento reológico dos nanofluidos; (iv) Analisar as características (tamanho, potencial zeta, turbidez, ângulo de contato e tensão superficial) dos nanofluidos, e; (v) Identificar a quantidade de óleo recuperada pela injeção de nanofluidos contendo sílica ou óxido de ferro em um leito poroso em escala laboratorial.

Metodologia

Os materiais utilizados na pesquisa foram: amônia, óleo mineral (MO) SAE 90 GL-5, cloreto de sódio (NaCl), dodecil sulfato de sódio (SDS), silicato de sódio neutro, NP de sílica comercial (CS-sílica), cinzas de casca de arroz e areia (300 e 600 μm). Além disso, foram utilizadas as nanopartículas de sílica sintetizada a partir da casca de arroz e precipitada do silicato de sódio. O método de moagem pra sintetizar a sílica a partir da casca de arroz (RH-sílica) foi adaptado da metodologia proposta por Agi et al. (2020), primeiramente, para remover a matéria orgânica, a casca de arroz foi calcinada a 800ºC por 7h na mufla, e então o material foi lavado com água destilada e filtrado a vácuo e depois foi seco na estufa a 100ºC por 15h, e então, pra obter um tamanho nano, o material foi moído em duas etapas, uma seca e uma úmida, A primeira moagem foi feita em um moinho de bolas por 4h, e a segunda moagem foi feita em um moinho de jarros em uma velocidade de 300rpm por 5h, após isso o material foi seco na estufa a 80ºC por 24h. Já o procedimento pra obter sílica utilizando o método de sol-gel (SG-sílica), foi baseado em 3 referências Maaref e et al. (2020); Chaturvedi, Sharma (2021); e Zulfiqar et al. (2016), inicialmente, foram adicionados 100ml de SS em um béquer e então foi colocado no ultrassom por 15 min, então 60ml de amônia foi adicionada lentamente e o béquer foi mantido no ultrassom por 1h, após isso o béquer ficou em repouso por 20 min e então foram adicionados 200 ml de água destilada e a solução ficou em repouso por mais 1h, o precipitado foi então filtrado e lavado com etanol e água destilada para remover os resíduos de amônia, por fim, o material foi seco na estufa a 250ºC por 30h. A preparação das soluções e nanofluidos foi realizada da seguinte forma: (i) a solução salina (B) foi preparada adicionando 3% de cloreto de NaCl em água destilada, com o auxílio de um agitador magnético, por 10 min; para a solução contendo NaCl e SDS (BS), primeiramente 0,12% do SDS foi adicionado em água destilada e a solução foi mantida em agitação magnética por 30 min, depois o NaCl foi adicionado e a solução ficou em agitação por mais 10 min, e; para preparar os nanofluidos, o mesmo procedimento foi realizado, mas após a segunda agitação, a porcentagem (0,10, 0,25, 0,50 e 0,75%) de nanopartícula foi adicionada e a solução foi mantida em agitação por mais 30 min, e então o nanofluido foi deixado no ultrassom por 1h. O mesmo procedimento foi realizado para cada uma das nanopartículas. A caracterização das nanopartículas foi realizada por meio da composição química (XRF), morfologia (TEM), grupos funcionais (FTIR), composição da

superfície química (XPS), área específica (BET) e distribuição de tamanho de poros. E, a análise dos nanofluidos foi realizada através da viscosidade, turbidez, tensão superficial, análise de tamanho de partícula e potencial zeta. Em relação ao sistema experimental, foi utilizado um béquer, uma bomba rotatória, um agitador magnético, uma coluna de leito fixo preenchida com 1058kg de areia e 950 ml de MO (que foi preparada antes de realizar cada teste) e então uma proveta, como recipiente para coleta. Por fim, os testes de recuperação foram realizados em três etapas, utilizando 4L de solução com um fluxo de inundação de 0,8 L/h, sendo a primeira etapa a inundação realizada com a solução B, a segunda com a solução BS e a última etapa a aplicação do nanofluido, após cada etapa a quantidade de óleo recuperado na proveta foi deixado em repouso por 24h para separação dos fluidos e então o volume foi medido, o mesmo procedimento foi realizado para cada uma das concentrações e tipo de NP.

Resultados e Discussão

Entre as Np, a RH-sílica apresentou a maior pureza entre as três amostras com 94,01 ± 0,26% em peso de SiO_2 e cerca de 5,99% em peso de impureza, incluindo K, Ca, P, Mg, Al, Mn, Fe, Zn, S, Zr e Ti. A CS-sílica apresentou uma pureza de 89,87 ± 0,33%, com uma quantidade razoável de Al e Na, e a SG-sílica apresentou a menor pureza, apenas 69,29 ± 0,51% de sílica, sendo que a maior parte da impureza, 26,79 ± 0,24% de Na, está relacionada ao precursor, o silicato de sódio. Em relação a estrutura cristalina, somente a RH-sílica foi caracterizada como cristalina, apresentando picos de cristobalita, tridimita e quartzo como polimorfos de sílica formados devido ao tratamento térmico, o tamanho do cristalino foi medido em 27 nm, a SG-sílica e a CS-sílica são amorfas. Todas as três amostras apresentaram estrutura esférica, com tamanhos de partículas medidos em 27 nm, 44 nm e 2453 nm, para CS-sílica, RH-sílica e SG-sílica, respectivamente. Quanto a área superficial e volume do poro, a CS-sílica foi caracterizada como mesoporosa, RH-sílica e SG-sílica apresentaram baixa área superficial e volume do poro. A análise dos grupos funcionais confirmou a existência de Si e O, os picos em 3436 e 953 cm^{-1} foram atribuídos aos grupos O-H das vibrações de estiramento presentes nos grupos silanol (Si-OH), a deformação de moléculas de água absorvidas na superfície das amostras apareceram no em 1635 cm^{-1}. Por fim, sobre a análise da superfície química das amostras, o oxigênio total (O1s) na superfície das amostras foi relacionado ao grupo siloxano Si-O-Si, os espectros de Si2p das amostras de sílica demonstraram a existência de SiO_2 puro, e o sódio (Na1s) apareceu em todas as superfícies, especialmente na SG-sílica, assim como foi apresentado na composição química. Em relação as análises dos nanofluidos, o tamanho e o potencial zeta foram medidos no primeiro dia e 30 dias depois, para analisar a estabilidade e aglomeração das partículas, de acordo com Setia e colaboradores (2013), um nanofluido com um potencial zeta maior que 30 mV e menor que -30 mV é estável e resiste à aglomeração, desta forma, CS-sílica e SG-sílica apresentaram estabilidade e resistência a aglomeração, e a RH-sílica apresentou uma estabilidade bem limitada, aumentou consideravelmente o tamanho da partícula, indicando aglomeração. A viscosidade em diferentes concentrações mostrou que a tensão de cisalhamento aumenta linearmente com o aumento da taxa de cisalhamento, indicando um comportamento newtoniano para os nanofluidos. Embora as nanopartículas sejam aglomeradas em nanofluidos CS e RH, a viscosidade do nanofluido diminui na ordem SG-NF > RH-NF a CS-NF, que segue uma ordem semelhante de tamanhos de nanopartículas. A tensão superficial é quase independente da concentração de nanopartículas para nanofluidos contendo

CS-sílica e SG-sílica e aumenta de acordo com a concentração de nanopartículas para nanofluido de RH-sílica. Por último, a análise da turbidez mostrou que as nanopartículas de CS e RH não parecem ter ficado retidas no leito de areia, porque a turbidez do nanofluido apresentou um ligeiro aumento após o teste de inundação (Mansouri et al., 2019), no entanto, as nanopartículas de SG ficam retidas no leito de areia, causando uma diminuição na turbidez. Em relação aos testes de inundações, a solução B apresentou uma recuperação média de 47,8 ± 5,9 % do óleo, a solução BS apresentou uma média de recuperação de 10,1 ± 1.5 %, a maior quantidade de óleo recuperado, 10%, foi obtido utilizando nanofluido contendo SG-sílica em uma concentração de 0,5%, o menor fator de recuperação, apenas 4,7%, foi obtido utilizando CS-sílica em uma concentração de 0.1% em massa. A maior quantidade de óleo recuperada com a RH-sílica foi de 8,9% do óleo, em concentração de 0.25% da NP, e a maior quantidade de óleo recuperada com a CS-sílica foi de 7,9%, em uma concentração de 0,75% de NP. O fator de recuperação obtido nessa pesquisa foi maior do que o relatado por Chaturvedi e Charma (2021) com nanofluidos contendo nanopartículas de sílica, e mais baixa que o obtido por Youssefvand et al. (2018), onde atingiram um valor mais alto, de 13,37% a 20,87% de recuperação de óleo usando Poliacrilamida Hidrolisada como aditivo no nanofluido à base de sílica. Por fim, foi possível observar que o fator de recuperação com nanofluido contendo sílica comercial aumenta à medida que a concentração de nanopartículas aumenta, devido ao aumento da viscosidade, conforme relatado por Lashari e Ganat (2020), nenhum efeito significativo da tensão interfacial foi observado para todos os nanofluidos, e os nanofluidos contendo CS-sílica e RH-sílica resultaram em fatores de recuperação semelhantes, indicando que a cinza da casca de arroz é um material promissor para produzir nanofluidos.

Considerações Finais
A viscosidade do nanofluido depende do tipo e da concentração do surfactante e não é modificada de forma significativa pelo tamanho da nanopartícula, e alguns estudos relatam que a viscosidade do NF deve ser próxima à do óleo para obter maior fator de recuperação. As características aparentes do NF dependem da interação e adsorção do tensoativo e da nanopartícula, o tamanho do NP não interfere muito no fator de recuperação em processos de EOR usando NF. A estabilização da espuma ajustando o tamanho do NP não tem influência direta no fator de recuperação. Sobre a molhabilidade e ângulo de contato: vários estudos relatam que os menores ângulos de contato não resultam em um alto fator de recuperação. Além disso, a injeção de nanofluidos em reservatórios rochosos tem demonstrado grande capacidade de alterar a tensão superficial e o ângulo de contato, o que influencia fortemente na eficiência da recuperação de petróleo. Em relação aos testes de recuperação, o ângulo de contato, viscosidade, tensão superficial e turbidez não mostram uma relação direta e significativa com o fator de recuperação. Por fim, quanto ao óleo recuperado, a melhor recuperação foi obtida com a sílica precipitada de silicato de sódio a 0,5% em peso, que recuperou 10% do óleo, e, o segundo melhor fator de recuperação foi obtido injetando a sílica sintetizada a partir de cinza de casca de arroz a 0,25%, que teve um fator de recuperação de 8,95%.

ABSTRACT

The use of nanofluids in enhanced oil recovery processes has gained attention due to the possibility to intensify the oil recovery from mature oil fields. Different mechanisms are involved when nanofluids are injected into oil wells, such as wettability alteration, reduction of interfacial surface tension, increase in the viscosity of the aqueous solution, and decrease in oil viscosity. Silica nanoparticles are extensively used for nanofluid formulations but there are important obstacles to the use of nanofluids in enhanced oil recovery. Stability is the most evident, in addition to environmental and economic aspects, and the need to design suitable large-scale production processes for the nanoparticle synthesis with the required characteristics. Thus, this study aims to evaluate the stability and efficiency of silica-based nanoparticles on enhanced oil. The effect of the silica nanoparticles from different sources (natural rice husk ash, sol,-gel silica, and a commercial silica sample), their characteristics, such as shape, size, concentration, water affinity, and their interactions with surfactant and oil, are discussed in terms of the oil recovery rate. The silica nanoparticles were well characterized using XRF, XRD, SEM, TEM, FTIR, XPS, and BET. The nanofluids with different nanoparticle concentrations were characterized according to their viscosity, surface tension, zeta potential, and stability. The oil recovery from an oil-saturated sand-packed bed increased due to the nanofluid injection after secondary recovery. An additional 5-10% oil recovery is achieved after flooding due to the injection of nanofluids, proving that silica from rice husk ash has comparable efficiency to other synthetic silica nanoparticles to be used in enhanced oil recovery.

Keywords: Nanofluids, Nanoparticles, Silica, Synthesis, Enhanced Oil Recovery.

FIGURE LIST

TABLE LIST

NOMENCLATURES

AAS – Alkyl Aryl Sulfonic acid

APS – Aminopropyldimethylethoxysilane

B – Brine solution

BET – Brunauer–Emmett–Teller

BJH – Barrett–Joyner–Halenda

BS - Brine with Surfactant solution

CS – Commercial Silica

CA – Contact Angle

CTAB – CetylTrimethylAmmonium Bromide

CVD – Chemical Vapor Deposition

DLS – Dynamic Light Scattering

EA – Ethoxylated Alcohol

EDTA – EthyleneDiamineTetraacetic Acid

EOR – Enhanced Oil Recovery

FTIR – Fourier-Transform Infrared Spectroscopy

IEP – IsoElectric point

IFT – Interfacial Tension

LA – Linear Alcohol

MO – Mineral Oil

MWCNT – Multi-Wall Carbon Nanotube

N-GQDs – Nitrogen-doped Graphene Quantum Dots

NF(s) – Nanofluid(s)

NP(s) – Nanoparticle(s)

OA – Oleic Acid

OOIP - Original oil in place

OS – Olefin Sulfonate

PAA – PolyAcrylic Acid

PAM – PolyAcrylaMide

PVP – PolyVinylPyrrolidone

RF – Recovery Factor

RH – Rice Husk silica

SDBS – Sodium DodecylBenzene Sulfonate

SDS – Sodium Dodecyl Sulfate

SLS – Sodium Lauryl Sulfate

SG – Sol-Gel silica

SS – Sodium Silicate

ST – Surface Tension

TEM – Transmission Electron Microscopy

XPS – X-ray Photoelectron Spectroscopy

XRD – X-ray Diffraction

XRF – X-Ray Fluorescence

SUMMARY

1 INTRODUCTION

Fossil fuels have been the world's leading energy source since the nineteenth century and are expected to remain so for several decades (NASR et al., 2021). World energy consumption is projected to increase by 50% by 2040. Despite the increased attention and considerable investments in renewable energy, energy demand is unlikely to be met entirely by renewable sources alone (SUN et al., 2020; YAKASAI et al., 2021).

Since fossil fuels are non-renewable energy sources, mature oil fields face a decline phase. It is estimated that 60% to 70% of the total oil remains in reservoirs when conventional hydrocarbon recovery techniques are employed (Kang et al., 2011), and several technologies have been proposed to improve oil extraction from existing reservoirs using EOR techniques (REZK and ALLAM, 2019a; SUN et al., 2020).

The oil recovery occurs in three steps: i) primary recovery; ii) secondary recovery; and iii) tertiary recovery, also known as enhanced oil recovery (EOR). In the primary recovery, the natural energy present in the reservoir is utilized, and 5-10% of the oil present in the reservoir is recovered. Water and gas are injected into the reservoir for secondary recovery, and the oil recovery is 10-55%.

Nevertheless, after the primary and secondary recovery, a large amount of oil remains in the pores of the reservoir due to the high capillary pressure of the water. Tertiary recovery techniques are applicable regarding the amount of oil still extractable from a reservoir, enabling an additional 5-15% of oil recovery from the reservoir. Different approaches are used to increase the efficiency by decreasing the ratio of mobility of the injected fluids, the interfacial surface tension between the fluid injected and the oil, the capillary forces, and changing the wettability of the reservoir (VISHNYAKOV et al., 2020) to allow the recovery of an additional 5-15% of oil from the reservoir (VISWANATHAN, 2017).

In this context, several studies have investigated the use of nanotechnology in EOR, some of which have successfully overcome the challenges of these techniques. Particularly, in chemical methods, the association between nanoparticles and surfactants used to prepare nanofluids for applications in EOR has been proposed by several authors over the latest years (AGI et al., 2020; ALI, H. et al., 2020; ALI, J.A. et al., 2020; SCHNEIDER, JOSÉ, MOREIRA, 2021; LAU, YU, NGUYEN, 2017). Surfactants are applied to reduce the interfacial tension between oil and water, making the displacement of the oil more efficient throughout the production pool. In addition, they can be added to the nanofluids to improve

their characteristics and properties. Although studies related to the application of nanofluids in the enhanced oil recovery are relatively recent, their utilization can improve the economy of the mature fields because the nanofluids can change the wettability of the rock surface, reduce the interfacial tension and the viscosity of the oil phase (SULEIMANOV, ISMAILOV, VELIYEV, 2011). The characteristics required for nanofluids to be applicable in EOR are defined during their production process and depend on the shape and size of the nanoparticles, concentration, additives, and hydrophilic/hydrophobic balance (ALI, J.A. *et al.,* 2020).

The method of preparing nanoparticles can play an essential role in controlling their physical and chemical properties, such as the size, morphology, and stability of the nanofluid (SAID et al., 2021). Some examples of widely accepted preparation methods for silica nanoparticles, like synthesis are hydrothermal (RAJ et al., 2019; CHEN et al., 2021), co-precipitation (SHALBAFAN et al., 2019; IZADI et al., 2019; SHALBAFAN et al., 2020), sol-gel (NEGI et al., 2021), chemical vapor deposition (SOLEIMANI et al., 2018), and biosynthesis (ZAMANI et al., 2020; OMIDI et al., 2020). Other less common methods have been also applied, such as Hummers (YOO, PARK, 2019), milling (AGI et al., 2020), and Stöber (WANG et al., 2010).

Silica nanoparticles are extensively used in enhanced oil recovery because they can be synthesized to present the desired characteristics for these processes (MITTAL, 2021, ZULFIQAR et al., 2016). Due to the high amount of silica required to produce nanofluids applicable in EOR, novel, cost-effective, and easy methods must be developed to produce nanoparticles (AGI et al., 2020). Sustainable methods and low-cost raw materials have been proposed in the literature, such as silica from rice husk ash, with several positive aspects. However, the effect of impurities, nanoparticles' size and shape, and nanofluid formulations are not completely understood.

Thus, this study aims to compare the efficiency of silica-based nanofluids in the enhanced oil recovery process and evaluate the effect of the silica nanoparticles' characteristics on the tertiary oil recovery.

2 OBJECTIVES

2.1 MAIN OBJECTIVES

The main objective of this study is to prepare and characterize silica-based nanoparticles and nanofluids and to evaluate the effect of silica-based nanofluids on enhanced oil recovery.

2.2 SPECIFIC OBJECTIVES

To achieve the main objective, the following specific objectives are proposed:

(i) Determine the chemical composition and surface chemistry of the nanoparticles.

(ii) Analyze the structure (morphology, crystalline structure, and microstructures), surface area, and pore size distribution of the nanoparticles.

(iii) Determine the rheological behavior of the nanofluids.

(iv) Analyze the characteristics (size, zeta potential, turbidity, and surface tension) of the nanofluids.

(v) Identify the amount of oil recovered by injecting nanofluids containing silica into a porous bed on a laboratory scale.

3 FUNDAMENTALS OF ENHANCED OIL RECOVERY AND APPLICATION OF NANOFLUIDS

This chapter presents the theoretical background and literature review for the application of nanofluids in enhanced oil recovery. Here, the main theoretical aspects and the state-of-art related to the enhanced oil recovery and nanofluid properties are discussed.[1]

3.1 INTRODUCTION

Nanotechnology is the area of science dedicated to the understanding of fundamental physics, chemistry, biology, and technology of objects at the nanometer scale (ALI, et al., 2018), whose concepts have been applied in several areas, such as engineering, chemistry, physics, biology, and medicine (MAMANI, 2009).
Nanofluids (NF) are colloidal suspensions obtained by dispersion of nanoparticles (NPs)
in a fluid (ethylene glycol, oil, water, saline solutions, and solutions containing surfactants, among others) (ALLOUHI; AMINE, 2021). The first applications of nanofluids in the oil and gas industry were in heat transfer systems and, more recently, their use has expanded to operations of drilling, completion, production, and Enhanced Oil Recovery (EOR).

Although studies on the application of nanofluids in enhanced oil recovery are recent, their use can improve the economics of mature fields. NF modifies rock surface wettability and reduces interfacial tension and oil phase viscosity (SULEIMANOV; ISMAILOV; VELIYEV; 2011). The modification of rock surface wettability leads to one of the most important characteristics of NF in EOR and will be discussed here in detail. Thus, the objective of this chapter is to present the state of the art of NP and NF preparation applicable to EOR and to discuss the main characteristics of NF necessary to achieve higher recovery rates.

3.2 ENHANCED OIL RECOVERY

---

[1] Partially published as "Aplicação de nanofluidos na recuperação avançada de petróleo – Uma revisão", in *Química: Ciência, Tecnologia e Sociedade*.
https://natal.uern.br/periodicos/index.php/QCTS/article/download/2436/2763

There are three methods of oil extraction: primary, secondary, and tertiary recovery (THOMAS, 2001). Tertiary recovery (or enhanced oil recovery, EOR) refers to the recovery of oil retained in the reservoir after the primary process, which uses pre-existing energies in the reservoir, and the secondary one, which consists of injecting water and/or gas into the reservoir (ALI, et al.,2018; AGI et al.,2020; THANG et al.,2020). In general, only 30 to 40% of the original oil in the reservoir is quickly recovered, with 60 to 70% of the oil remains trapped in the reservoir's pores and channels. Thus, increasing production by only 5% still represents a major challenge for conventional EOR processes (ALI, et al., 2020; AGI et al., 2020; THANG et al., 2020).

For tertiary recovery, several methods are used, including chemical, thermal, and miscible. Thermal methods are intended to decrease the viscosity of the oil (by increasing the temperature). The high viscosity hinders its mobility between the pores and the displacement of the oil to the production wells (THOMAS, 2001).

Chemical methods consist of injecting products that can chemically interact with the fluid present in the reservoir, such as solutions containing polymers, and alkaline solutions (LIU et al., 2020). Solutions containing polymers can reduce the interactions between the oil with high viscosity and the porous medium of the reservoir, thus increasing the mobility and displacement of the mixture (oil and polymeric solution) to the production wells. The injection of alkaline solutions, on the other hand, enables reactions with organic acids present in the reservoir, producing surface-active substances (LIU et al., 2020; THOMAS,2001)

There are numerous recent works and review articles published dealing with enhanced oil recovery using biological methods (GEETHA, et al., 2018; SAFDEL, et al., 2017; GAO, 2018; SARAVANAN et al., 2020; JEONG, et al., 2017; GAO, 2018; SARAVANAN et al., 2020; JEONG, et al. .,2019) with the use of polymers (EL-HOSHOUDY et al.,2017; AFOLABI et al., 2019; AFOLABI et al., 2018; DRUETTA et al., 2019), steam (DONG et al., 2019), nanoparticles (NEGIN; ALI; XIE, 2016; OLAYIWOLA; DEJAM, 2019), ultrasound (WANG; GUO, 2019), chemical methods (DRUETTA et al., 2019; ESENE et al., 2019; TACKIE-OTOO et al., 2020), CO_2 injection (KUMAR; MANDAL, 2017; SONG, et al., 2020), electromagnetic nanofluids (ALI, et al., 2020), and polymeric nanofluids (LASHARI; GANAT; 2020; GBADAMOSI, et al., 2018). Thus, there is not only one solution for tertiary recovery, so it must be analyzed on a case-by-case approach (YUAN; WOOD, 2018).

3.3   APPLICATION OF NANOFLUIDS IN EOR

Nanoparticles have unique characteristics that make them efficient in EOR. Their small size allows their permeation into the pores of reservoir rocks (GBADAMOSI, et al., 2018), causing the release of oil. In addition, they can trap hydrocarbon molecules and drag them to the surface (THANG et al., 2020, 2012). The literature reports several nanofluid formulations, but there is no consensus on the ideal formulation for each type of oil and reservoir (Table 3.1). However, the viscosity and density of the oil seem to be the most important characteristics in the selection and formulation of the nanofluid. The correlation between the formulation and recovery factor of the oil is presented in section 3.5.

For applications in EOR, NPs must meet the following specificities (LAU; YU; NGUYEN, 2017):

(i) Change the wettability of rocks and reduce the interfacial tension between water and oil. Due to their small dimensions, NPs can pass through the pores in the reservoirs, reaching the residual oil. The change in rock wettability and the reduction of interfacial tension occur due to its surface characteristics, reducing the capillary force necessary for the oil phase to be displaced.

(ii) Reduce the viscosity of the oil and improve the viscosity of the injection fluid: The presence of nanoparticles in the injected fluid modifies the fluid's viscosity and improves the mobility of the oil in the reservoir, which increases the macroscopic recovery factor (RF).

The actions of the nanofluid are described by the following mechanisms:

(i) Improvement of the thermal conductivity of the heavy oil: The addition of nanoparticles can result in an increase in the thermal conductivity and the specific heat of the reservoir, in addition to modifying the density and viscosity of the fluids applied to the EOR.

(ii) Modification of the characteristics of heavy oil in situ: Among the changes in the characteristics of heavy oil, the presence of some types of nanoparticles, such as nickel, copper oxide, and zinc oxide, in addition to changing wettability, and decrease the viscosity of oil in reservoirs, can act as catalysts for hydrogenation and cracking reactions.

Table 3.1. Important features of oil reservoirs where EOR has been applied.

Oil or Model Compound	M (mPa·s)	ρ (g/cm³)	Components	Reference
1-Bromodecane	-	-	-	Jha et al., 2020
n-Decane (Etra Dry, AcroSeal)	2.80	0.81	Asphaltene: 0.45%	Kuang et al., 2018
n-Decane	-	-	-	Rezk et al., 2019
n-Octane	-	-	-	Tabar et al., 2020
Mineral oil (Keratech 24 MLP)	24	-	-	Nourafkan et al., 2018
Mineral oil (Synfluid®, PAO 6 cSt)	-	-	-	Maarefet al., 2020
Crude oil	20.2	-	Asphaltene: 3.6%; Sulphur: 2.24; H2S: 153 ppm; wax: 5.4%	Jalilianet al., 2019
Crude oil	141.2	0.94	-	Divandari et al., 2019
Crude oil	7.6	0.85	Saturated: 53%; Aromatics 35%; Resin: 12%; Asphaltene: 0.90%	Rognmo; Heldal; Ferno, 2018)
Crude oil	2.28	-	-	Zhou et al., 2020
Crude oil	2.73	0.85	-	Xu et al., 2019
Crude oil	3.43	-	-	Wu et al., 2020
Crude oil	100	0.86	Resin: 14.6%; Wax: 39.13%; Asphaltene: 1.02%; Sulphur: 0.06%; Alkane: 45.79%	Raj et al., 2019
Crude oil	11	0.88	-	Asl et al., 2020
Crude oil	39	0.90	-	Shalbafan et al., 2019
Crude oil	35	0.83	-	Radnia et al.,2018
Crude oil	-	0.87	-	Soleimani et al., 2018
Crude oil	39	-	-	Kumar et al., 2017
Crude oil	6.11	0.84	-	Mohajeri et al., 2019
Crude oil	-	-	Saturated: 53.12%; Aromatics 28.13%; Resin:	Giraldo et al., 2019

			18.24%; Asphaltene: 0.22%	
Dehydrated crude oil mixed with kerosene	5	0.82	-	Zhao et al., 2018
Intermediate crude oil	117.6	-	Saturated: 53.9%; Aromatics 26.25%; Resin: 53.9%; Asphaltene: 7.7%	Betancur et al., 2020
Light crude oil	1.4	-	Saturated: 42.82%; Aromatics 13.81%; Resin: 42.32%; Asphaltene: 1.05%	Franco-Aguirre et al., 2018
Heavy crude oil	160	-	Saturated: 41%; Aromatics 49%; Resin: 2%; Asphaltene: 8%	Panahpoori et al., 2019

The addition of NP to specific fluid mixtures (such as ethylene glycol, oil, water, saline solutions, and solutions containing surfactants, among others) produces a nanofluid (NF) with different properties and characteristics. When applied to EOR, NFs can build ordered structures, such as wedge-shaped films, at the solid-oil interface, which results in NF scattering on the surface (Figure 3.1) (ALI, et al.,2020).

Figure 3.1 Structure formed by the NF in the EOR.
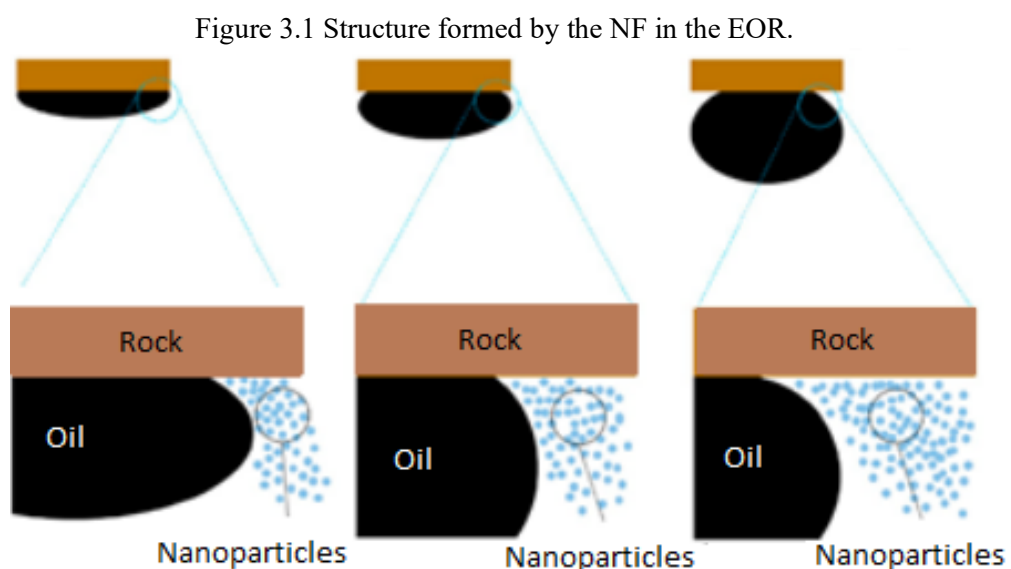
This process occurs due to the disjoining pressure, that is, a disconnected or separation pressure, one of the main phenomena that influence the formation of evaporation films and the magnitude of the contact angle. Separation pressure is a phenomenon that happens in thin liquid films when an ultrathin liquid film encounters a solid surface. There

is an attraction between the molecules of the liquid phase and those of the solid phase, where the pressure in the liquid needs to balance the pressure of the environment and the attractive forces between solid and liquid, but when the film is very thin, the attractive forces act to push the liquid away. This force is called the separation pressure. The separation pressure is related to the ability of the fluid to spread across the surface of a substrate due to the difference in interfacial forces between oil and solids, induced by NP (ALI, et al.,2020; FAGHRI; ZHANG, 2006).

On the other hand, NPs can cause a blockage in the pore channel, giving rise to a phenomenon called "mechanical entrapment", which occurs when the throat or pore size is smaller than the NP pore size. NP or when NP accumulates as NF flows through the pores, due to the increased velocity of NF. This is caused by the narrowing of the pores caused by the NP attached to pore walls. Blockage of the pores causes pressure in neighboring pores, pushing out the oil droplets trapped in them (ALI, et al., 2020).

3.3.1 Nanoparticles applied in EOR

Table 3.2 summarizes the main types of nanoscale materials and their characteristics used in the preparation of NF applicable to EOR. The dominant mechanism of action of nanoparticles on the EOR depends on the physicochemical characteristics of the nanoparticles, and can be classified according to their action in (NEGIN; ALI; XIE, 2016):

(i) Reduction of oil viscosity: Al_2O_3, CuO, Fe_2O_3/Fe_3O_4, Ni_2O_3, MgO, polymer-coated nanoparticles, among others;

(ii) Reduction of oil-water interfacial tension: SiO_2, Hydrophobic and Lipophilic Polysilicon (HLP), polyacrylamide nanospheres, polymer-coated nanoparticles, ferrofluid;

(iii) Alteration wettability: SnO_2, SiO_2, SiO_2 coated with Al_2O_3, hydrophobic silica, nanoparticles coated with polymers;

(iv) Scanning and displacement efficiency: polymeric nanoparticles; nanoparticles coated with polymers, among others

Table 3.2 Relationship between hydrophilic/hydrophobic characteristics and size of the NP

NP	Characteristic	Size (nm)	Surface area (m²/g)	Shape	Reference
SiO_2	Partially hydrophobic	137.2	364 ± 6	-	Maaref et al., 2020
PSBT+PSMA*	-	27.1 ± 1.9	-	-	Zhou et al., 2020
Quantum dots – graphene	-	2 to 5	-	-	Tabar et al., 2020
ZrO_2	-	100	-	-	Jha et al., 2020
SiO_2	-	20 to 30	-	-	Asl et al., 2020
SiO_2-C_{12}	Amphiphilic	40	-	-	Wu et al., 2020
SiO_2	Hydrophilic	30	-	-	Wu et al., 2020
NP iron-carbon Nucleo	-	60	123	-	Betancur et al., 2020
TiO_2	Hydrophilic	20	$10 \sim 45$	-	Panahpoori et al., 2019
ZrO_2	-	≤ 100	≥ 25	-	Jalilian et al., 2019
Fe_3O_4 covered with SLS	Hydrophilic	44 to 50	-	-	Shalbafana et al., 2019
Fe_3O_4 covered with EDTA	Hydrophilic	20 to 25	-	-	Shalbafana et al., 2019
MoS_2	Hydrophilic and hydrophobic	100	-	-	Raj et al., 2019
SiO_2	-	20	-	-	Xu et al., 2019
Fe_2O_3	Hydrophilic	50 to 80	-	Spherical	Divandari et al., 2019
Fe_3O_4 covered with nitric acid	Hydrophilic	-	-	Spherical	Divandari et al., 2019
NiO/SiO_2	-	116.5	22		Giraldo et al., 2019
SiO_2	-	94 ± 4	24	Spherical	Giraldo et al., 2019
SiO_2	Hydrophilic	15	-		Mohajeri et al., 2019
ZnO	Hydrophilic	50 ± 20	-	Spherical	Rezk et al., 2019
Grafeno-DSu	Amphiphilic	0,31	-	-	Radnia et al., 2018

SiO₂	Hydrophobic	14-16	380	-	Zhao et al., 2018
TiO₂		21		Spherical	Nourafkan et al., 2018
Carbon nanotubes	-	16-20	-	Cylinder	Soleimani et al., 2018
SiO₂	Hydrophilic	15 ~ 20	-	Spherical	Kuang et al., 2018
Al₂O₃	Hydrophobic	< 50	-	-	
SiO₂	Hydrophilic	23,3	-	Spherical	Rognmo et al., 2018
SiO₂	Hydrophilic	20,3	-	-	
SiO₂	Hydrophilic	7	380	-	Franco-Aguirre et al., 2018
SiO₂	Hydrophilic	11 ~ 14	-	-	Yousefvand et al., 2018
SiO₂	Hydrophilic	40		Spherical	Kumar et al., 2017

*PSBT+PSMA: Poly[(9,9-dioctylfluorenyl-2,7-diyl)-alt-co-(1,4-benzo-{2,1′,3}-thiadiazole)]+Poly(styrene-co-maleic anhydride)

Silica NPs were the most explored in the formulation of NF applied to tertiary oil recovery. Although there is no consensus, hydrophilic or slightly hydrophilic materials, such as hydrophilic SiO₂, have a greater potential for EOR, being up to 40% higher than hydrophobic $SiO2_2$ (ROGNMO; HELDAL; FERNO, 2018). The concentration of NP in the formulation of an applied NF the EOR is usually in the range of 0.005% and 3% (by mass), as will be discussed in Chapter 4 of this work.

The properties and characteristics of NP vary according to the method of preparation, among them: inert gas condensation, the sol-gel process, chemical vapor deposition (MAMANI, 2009; OLIVEIRA, 2012), coprecipitation processes, and solvent evaporation (ALI, et al., 2020), among others. The first method used, and still the most common today, is solvent evaporation. This method uses high-speed homogenization or ultrasonic agitation, followed by solvent evaporation, through continuous magnetic agitation at elevated temperatures or reduced pressure, resulting in the formation of nanometric particles (ALI, et al., 2020). In the inert gas condensation method, the material is vaporized in a vacuum chamber and then the vapor is condensed into NP by collision with an inert gas fluid at controlled pressure.

In the sol-gel method, the solution forms a two-phase system and allows controlling all stages of the synthesis process, obtaining materials with pre-defined

characteristics (MAMANI, 2009; OLIVEIRA, 2012). In Chemical Vapor Deposition (CVD), a substrate is exposed to one or more volatile precursors, which react or decompose on the substrate surface, producing the desired deposit (OLIVEIRA, 2012). In coprecipitation, the synthesis is carried out through the mixture of inorganic salts in an aqueous medium and then precipitation with alkali hydroxide is carried out. This method has advantages such as chemical homogeneity, low reaction temperature, synthesis of particles of uniform sizes, and, little or no agglomeration of NP (MAMANI, 2009). To produce NP with a scale of pre-defined dimensions, the method of fractionation of the colloidal suspension, such as centrifugation and size exclusion chromatography, can also be used. In this case, particles of different dimensions are separated through density or size (MAMANI, 2009).

After the synthesis of nanoparticles, the formulation and preparation of the nanofluid (NF) follow typical procedures (OLIVEIRA, 2012):

(i) directly with the dispersion in the base fluid, in a single step, where the evaporation of the NP is carried out in a vacuum and then its condensation in the base fluid. This method reduces the agglomeration of the NPs but has a high operational cost.

(ii) In two steps: first, the synthesis of the NP is carried out, and then the powder is dispersed in the base fluid. The dispersion of NPs in the base fluid can be carried out through the high-pressure homogenization process, where the NPs are pressurized so that they have enough energy for the agglomerations to be broken and then dispersed in the base fluid. Alternatively, the dispersion can be carried out by ultrasonic agitation. The two-step method has a lower operating cost, facilitating a large production scale, and it is possible to obtain a greater variety of NF, with different base fluids, NP, and NP sizes. However, it usually produces a greater agglomeration of NPs.

3.3.2 Surfactants Applied in EOR

Anionic surfactants are already widely used in EOR, due to their lower adsorption on reservoir rocks when compared to other groups of surfactants (ALI, et al., 2018; ALNARABIJI; HUSEIN, 2020). Among the anionic surfactants, carboxylates, sulfonates, sulfates, and phosphates stand out (DALTIN, 2011).

Although the nanofluids applied in EOR usually contain a surfactant in their formulation, several works demonstrate that it is possible to use a nanofluid without a surfactant (ALNARABIJI; HUSEIN, 2020). In any case, the NP parameters that define the

nanofluid efficiency are NP size and size distribution, surface charge, isoelectric point (IEP), concentration, and physicochemical properties. However, in most studies, an agent used is also used in the formulation of NF. The addition of surfactants to NF can reduce the agglomeration of NP, decreasing the interfacial tension between the base fluid and NP, but as a result, they change the thermal characteristics of the solution or suspension (OLIVEIRA, 2012).

A single surfactant or combination of more than a type of surfactant can be used for NF formulation (Table 3.3). The most commonly used are Alkyl Aryl Sulfonic acid (AAS); Oleic Acid (OA); Polyacrylic Acid (PAA); Ethoxylated Alcohol (EA); Linear Alcohol (LA); Alkyl ammonium; Benzalkonium chloride; Cetyl Trimethyl Ammonium Bromide (CTAB); L-Arginine; L-Cysteine; N-alkyl betaine; Sodium DodecylBenzene Sulfonate (SDBS); Sodium Dodecyl Sulfate (SDS); Polysorbate 80 (Span80); Olefin Sulfonate (OS); Propoxysulfate; Tween 80 (TW-80); Triton -100 (T-100).

The addition of NP to solutions containing surfactants can stabilize the formation of foams (CHATURVEDI; SHARMA, 2021), as the NPs adhere to the liquid-bubble interface, keeping the two interfaces separate. The smaller the size of the NP, the greater the stability of the foam formed.

When there is a mixture of surfactants, they have an adsorbed surfactant layer containing alternating charges (positive and negative), which confers great cohesion. This is due to: (i) efficient packing at the interface, (ii) the right amount of free surfactant in solution, and (iii) the formation of vesicles in thermodynamic equilibrium, which provides viscoelastic properties within the solution and, therefore, good stability to the foams. The concentration of surfactant added to NF generally used is in the range of 0.01 to 7 w/t% (DALTIN, 2011; CHATURVEDI; SHARMA, 2021).

Injecting surfactants into reservoirs reduces the interfacial tension between water and oil (LIU et al., 2020; DALTIN, 2011), which reduces the capillary pressure of the pores, thus allowing water to displace residual oil. So, the lower the interfacial tension, the more oil can be recovered. However, the use of surfactants in EOR can generate foam, a major problem that must be removed from wastewater, so that the environmental impact is reduced (ALNARABIJI; HUSEIN, 2020).

Table 3.3. Type of nanoparticles and surfactant used in the formulation of the NF

NP	Surfactant	Surfactant's characteristic	Reference
SiO_2	Span 80	Non-ionic	Maaref et al., 2020
SiO_2	L-arginine	Amphoteric	Asl et al., 2020
	L-cysteine		
Polymer	N-alquilbetaine	Amphoteric	Zhoua et al., 2020
Graphene – N dopped	CTAB	Cationic	Tabar et al., 2020
ZrO_2	SDBS	Anionic	Jha et al., 2020
SiO_2-C_{12}	CTAB	Cationic	Wu et al., 2020
SiO_2			
Iron with carbon Nucleo	Propoxysulfate	Cationic	Betancur et al., 2020
TiO_2	CTAB	Cationic	Panahpoori et al., 2019
ZrO	T-100	Non-ionic	Jalilian et al., 2019
Fe_3O_4	TW-80	Non-ionic	Shalbafana et al., 2019
Fe_3O_4 + EDTA			
MoS_2 nanosheets	SDS	Anionic	Raj et al., 2019
Fe_2O_3	SDS	Anionic	Divandari et al., 2019
NiO/SiO_2	CTAB	Cationic	Giraldo et al., 2019
SiO_2			
ZnO	SDS	Anionic	Rezk et al., 2019
G-DSu	SDBS	Anionic	Radnia et al., 2018
SiO_2	T-100	Non-ionic	Zhao et al., 2018
Carbon nanotubes	SDS	Anionic	Soleimani et al., 2018
Al_2O_3	Poly(acrilic acid)	Anionic	Kuang et al., 2018
	Linar alcohol	Non-ionic	
SiO_2	Alkyl ammonium	Anionic	
	Ácido oleic	Anionic	
SiO_2	KD	Anionic	Xu et al., 2019
SiO_2	LA ethoxylated	Non-ionic	(Rognmo; Heldal; Ferno, 2018)
SiO_2	Silnyl® FSJ	Anionic	Franco-Aguirre et al., 2018
SiO_2	SDBS	Anionic/zwitterionic	Kumar et al., 2017
TiO_2	(AAS) + (EA)	Non-ionic	Nourafkan et al., 2018
SiO_2	SDS	Anionic	Yousefvand et al., 2018; Mohajeri et al., 2019

3.4 NANOFLUID CHARACTERIZATION

The characterization of an NF comprises the knowledge of its rheological, optical, and surface tension properties.

3.4.1 Interfacial tension

The interfacial tension of crude oil and injected NF is one of the main parameters to determine the movement and distribution of fluids in porous media, such as reservoir rocks (SÁ; SERRUYA; FERREIRA, 2018; ALI, et al., 2020). In the case of EOR, the injected NF must have low interfacial tension, otherwise, the fluid's ability to repel oil from the pores is low, resulting in low oil recovery (ALNARABIJI; HUSEIN, 2020). According to Table 3.4, the NF interfacial tension lies in the range of 0.0006 to 45 mN/m, and it is determined by the type and concentration of surfactant used in the formulation.

Table 3.4. Interfacial tension (IFT) of some nanofluids used in EOR.

NP	Surfactant	IFT (mN/m)	Reference
SiO_2	Span 80	34.03	Maaref et al., 2020
Quantum dots graphene-N	CTAB	4.69 to 15.72	Tabar et al., 2020
TiO_2	CTAB	0.9 to 3.5	Panahpoori et al., 2019
MoS_2	SDS	0.2 to 0.8	Raj et al., 2019
SiO_2	KD	0.0006 to 0.0204	Xua et al., 2019
Fe_3O_4 covered with nitric acid	SDS	16.71 to 22.35	Divandari et al., 2019
NiO/SiO_2 s	CTAB	17	Giraldo et al., 2019
SiO_2		20.5	
ZnO	SDS	7.1	Rezk et al., 2019
Graphene-DSu	SDBS	12.92 to 14.49	Radnia et al., 2018
TiO_2	AAS + EA	10.5 to 13.2	Nourafkan et al., 2018
Carbon nanotubes	SDS	31.17 to 33.46	Soleimani et al., 2018
SiO_2	Silnyl® FSJ	18.1	Franco-Aguirre et al., 2018
SiO_2	SDS + HPAM	2.46 to 3.20	Yousefvand et al., 2018
SiO_2	Alkyl ammonium	17	Kuang et al., 2018
	OA	45	
	PAA	27	
	Linear alcohol	8	

Al$_2$O$_3$	OA	38	
	PAA	29	
	Linear alcohol	8	
SiO$_2$	SDBS	30.1 to 33.0	Kumar et al., 2017

3.4.2 Wettability

Wettability affects the permeability curves, capillary pressure, dispersion, irreducible water saturation, and the displacement and reduction in oil saturation (ALI, et al., 2018). Compounds that have high surface tension tend to form spherical drops on the surfaces, presenting low wettability, due to a strong attraction between the molecules causing them to stick together. In compounds that have a low interfacial tension, the fluid tends to spread across the solid surface (DALTIN, 2011). Therefore, when a surface is highly wetted by water, the formed drop tends to spread, and consequently, have a low contact angle (ALI, et al.,2018). When hydrophilic nanoparticles are injected into the porous medium, they tend to increase the relative permeability of the oil phase, because they cause the reservoir to become highly humid, changing its wettability (JU; LI, 2012). In this way, there will be an increase in oil recovery in flooded reservoirs (ALI, et al., 2020).

3.4.3 Rheological behavior

For EOR using nanofluids, the viscosity of NF must be similar to the viscosity of petroleum. If the viscosity of the injected fluid is much lower than that of the oil, the NF will flow more easily between the pores, towards the production wells, leaving the oil behind, resulting in low Recovery Factor (RF) (ALNARABIJI; HUSEIN, 2020). In general, the viscosity of NF used in EOR is in the range of 0.485 mPa·s to high values (230 mPa·s) (Table 3.5).

Table 3.5. Viscosity of different NF utilized in EOR.

NP	d_{NP} (nm)	[NP] (ppm)	Surfactant	[Surfactant] (ppm)	μ (mPa·s)	Reference
SiO$_2$	20 to 30	100 to 1000	L-arginine	2000	1.23	Asl et al., 2019
	100		L-cysteine	4500	1.35	
MoS$_2$	116.5	50 to 100	SDS	1000	110 to 230	Raj et al., 2019
NiO/SiO$_2$	94 ± 4	100	CTAB	9	1.21	Giraldo et al., 2019
SiO$_2$	15 to 20	100 to 1000			1.09	
SiO$_2$		1000	Linear alcohol		0.49	Kuang et al., 2018

3.5 EXTRACTION YIELD IN ENHANCED OIL RECOVERY USING NANOFLUIDS

Recovery Factor (RF) is the ratio between the volume of recoverable oil and the original volume of fluid in a reservoir, which is not a constant value, due to the different characteristics presented by each reservoir (SÁ; SERRUYA; FERREIRA, 2018).

The concentration of NP plays an extremely important role in the process because when increasing the concentration of NP, the separation pressure tends to increase, which causes an increase in repulsive forces (LASHARI; GANAT; 2020). However displacement efficiency improves with increasing NP concentration, due to increased viscosity, reduced interfacial tension in reservoir fluids, and large change in wettability at the rock surface (LASHARI; GANAT; 2020). On the other hand, the literature reports that the concentration of NP is not directly related to viscosity and, consequently, to RF. Based on these observations, a higher concentration could be promising in improving recovery rates.

The highest RF reported in the literature (87.1%) (Table 3.6) was obtained when NP of partially hydrophobic silica (0.5 wt%) and the non-ionic surfactant Span 80 (0.5 %) were used to recover mineral oil (Synfluid®, PAO 6 cSt). However, this result cannot be generalized, since it also depends on the type of oil and characteristics of the reservoir.

Although the formulation of an NF varies, in general, the concentration of NP and surfactant that maximizes recovery is of the order of 0.1-0.5 wt% and 0.1-0.2 wt%. However, to optimize recovery, experimental design can be suggested, also considering the type of reservoir and oil properties. The surfactant concentration used in the NF

formulation is generally in the range of 0.1% to 8% (by mass), but the highest recovery factors are achieved when the surfactant concentration is in the range of 0.1% to 0.5%.

It is important to emphasize that the total RF includes primary, secondary, and tertiary recovery and that the literature does not always report recovery factors at each stage. About the tertiary RF obtained through the injection of NF, the average of the RF is 18.77%.

In some cases, the influence of different concentrations of NP and/or surfactants on the RF, it is possible to observe that the RF is higher when the surfactant concentration is higher than 0.2 m/m% and the NP concentration is lower, 0.1% (by mass) (MOHAJERI, et al., 2019). Table 3.6 also shows the relationship between the size of the NP and the recovery factors.

The foam stabilization ability is also affected by the size of the NP present in the NF, and the smaller the size of the NP, the more stability the foam will have. The size of the nanoparticles must be such that it is not too large so that it does not get stuck in the pores causing clogging and not too small so that it does not cause extra clogging in the pores (ALI, et al., 2020). However, the concentration of nanoparticles in the nanofluid is the main factor that affects the injection of nanofluid into porous media to improve oil recovery (ALI, et al., 2020). If the limit of 3 m/m% is exceeded, there will be retention of nanoparticles in porous media causing a decrease in porosity and permeability of the medium due to pore blockage (ALI, et al., 2020).

The NF injected into the reservoirs must have a low value of interfacial tension (ALNARABIJI; HUSEIN, 2020), so that the NF will be able to repel oil from the pores more effectively, and consequently will have a higher RF. As shown in Table 3.6, when the interfacial tension is lower (0.9 to 3.5mN/m), it results in higher RF (for tertiary recovery only) between 24% and 36%. On the other hand, when the interfacial tension is high (ALI, et al., 2020) (4.69 and 15.72 mN/m), the RF is lower (15% to 22%). At lower surface tension, the contact angle decreases, which increases the wettability of the rock, as also shown in Table 3.6, i.e., the smaller the contact angle, the higher the FR. This greater surface interaction also modifies the adsorption characteristics of the surfactant on the NP, and the greater the surfactant adsorption capacity on the surface of the NP, the higher the tertiary recovery factor.

Table 3.6. Recovery factors were obtained with the use of nanofluid of different formulations and its characteristics.

NP	[NP] (m/m%)	d_{NP} (nm)	Surfactant	[Surfactant]	IFT (mN/m)	CA	Oil	RF*	Reference
Polymer	0.05 %	27.1 ± 1.9	N-alkylbetaine	0.1 wt%		101.3°	Crude oil	11.47%	Zhou et al., 2020
Quantum dots graphene	0.01 %	2 to 5	CTAB	0.3 wt%	4.69 to 15.72	64.57° to 69.47°	n-Octane	22%	Tabar et al., 2020
	0.005 %							15%	
ZrO$_2$	0.01 %	100	SDBS	1.435 mM	-	-	1-Bromodecane	55.35	Jha et al., 2020
	0.10 %							17.4%	
SiO$_2$-C$_{12}$	0.005 %	40	CTAB	-	-	63°	Crude oil	13.46%	Wu et al., 2020
	0.01 %							15.74%	
	0.02 %							16.36%	
SiO$_2$	0.01 %	30						3.64%	
Iron-carbon Nucleo	-	60	SO + propoxysulfate	-	-	0.03°	Intermediate crude oil	84% (total)	Betancur et al., 2020
TiO$_2$	0.01 %	20	CTAB	0.01 wt%	0.9 to 3.5	20° to 40°	Heavy crude oil	24%	Panahpoori et al., 2019
	0.03 %			0.03 wt%				36%	
	0.06 %			0.06 wt%				24%	
	0.1 %			0.1 wt%				24%	
TiO$_2$	2000 ppm	21	(AAS) 25% + (EA) 75%	0.3 wt%	10.5 to 13.2	-	Mineral oil (Keratech 24 MLP)	7.81%	Nourafkan et al., 2018
ZrO	0.01g	≤ 100	T-100	0.015 mL	-	-	Crude oil	60% (total)	Jalilian et al., 2019

Fe$_3$O$_4$ covered with SLS	0.3 %	44 to 50	TW-80	0.5 wt%	-	3.85º	Crude oil	20%	Shalbafan et al., 2019
Fe$_3$O$_4$ covered with EDTA	0.2 %	20 to 25						13.49%	
MoS$_2$	0.005 % / 0.010 %	100	SDS	0.1 wt%	0.2 to 0.8	18°	Crude oil	19.71% / 19.07%	Raj et al., 2019
Fe$_2$O$_3$		50 to 80	SDS	-	-	-	Crude oil	11%	Divandari et al., 2019
Fe$_3$O$_4$ covered with citric acid	-	-			16.71 to 22.35			22%	
NiO/SiO$_2$	100 mg/L	116.5	CTAB	9 mg/L	17	19º	Crude oil	60% (total)	Giraldo et al., 2019
SiO$_2$	100 mg/L / 1000 mg/L	94			20.5	28°		42% (total) / 48% (total)	
ZnO	0.05	50 ± 20	SDS	0.2 wt%	7.1	-	n-Decane	35%	Rezk et al., 2019
G-DSu	0.5 mg/mL / 2 mg/mL	0.31 (grafeno)	SDBS	1 g	12.92 to 14.49	103° to 148°	Crude oil	8% / 14%	Radnia et al., 2018
CNT	0.05 % / 0.30 % / 0.40 %	16.8 to 20.61	SDS	-	31.17 to 33.46	-	Crude oil	12.22% / 18.57 % / 14.44 %	Soleimani et al., 2018
SiO$_2$	0.1 %	15 to 20	Alkyl ammonium	-	17	13º	n-Decane	45% (total)	Kuang et al., 2018
			AO		45	150º		41.5% (total)	
			PAA		27	10º		45% (total)	

Nanoparticle	Concentration	Size	Surfactant	Surfactant Conc.	IFT	Contact angle	Oil	Recovery	Reference
			Linear alcohol		8	130º		48.5% (total)	
Al$_2$O$_3$	0.1 %	< 50	AO		38	120º		40% (total)	
			PAA		29			44% (total)	
			Linear alcohol		8	50º		47.5% (total)	
SiO$_2$	5000 mPPM	23.3	Linear alcohol ethoxylated	10.000 mPPM	-	-	Crude oil	15.4%	Rognmo; Heldal; Ferno, 2018
	1500 mPPM							14.1%	
SiO$_2$	1500 mPPM	20.3						10.1%	
SiO$_2$	500 mg/L	7	Silnyl® FSJ	0.46 wt%	18.1	79° to 128º	Light crude oil	31.8%	Franco-Aguirre et al., 2018
SiO$_2$	0.25 %	11 to 14	SDS + HPAM	0.12 wt% + 0.8 wt%	2.46 to 3.20	104°	Heavy oil	30%	Yousefvand et al., 2018
	0.5 %							35%	
	0.75 %							37.5%	
	1.00 %							31.25%	
SiO$_2$	0.2 %	40	SDBS	0.0825 wt%	30.1 to 33.0	-	Crude oil	24.81%	Kumar et al., 2017
SiO$_2$	0.5 %	137.2	Span 80	0.5 wt%	34.03	51.4º	Mineral oil (Synfluid®, PAO 6 cSt)	87.1% (total)	Maaref et al., 2020
SiO$_2$	0.01 %	20.56	KD	0.05 wt%	0.0006 to 0.0204	36º to 78º	Crude oil	18.16%	Xua et al., 2019
	0.03 %							21.56%	
	0.05 m/m%							19.40%	
SiO$_2$	0.1 %	14 to 16	T-100	0.1 wt%	-	-	Dehydrated crude oil	16%	Zhao et al., 2018

							mixed with kerosene		
SiO$_2$	1000 ppm	20 to 30	L-arginine	0.2 wt%	-	14.5° to 18°	Crude oil	12.7%	Asl et al., 2020
			L-cysteine	0.45 %				13.1%	
SiO$_2$	0.1 %	15	SDS	0.2 wt%	-	-	Crude oil	71% (total)	Mohajeri et al., 2019
	0.02 %							78% (total)	
	0.1 %			0.1 wt%				59% (total)	
	0.02 %							67% (total)	

*When the paper presents more than one RF, the table shows average values.

Table 3.7 shows the relationship between the viscosity of NF and the FR, where it is possible to observe that the closer the NF viscosity meets the oil viscosity, the greater the FR.

Table 3.7. Relationship between NF, viscosity, and RF.

NP	Surfactant	μ NF (mPa·s)	μ oil (mPa·s)	RF*	Reference
SiO$_2$	L-arginine	1.22 to 1.25	11	12.7%	Asl et al., 2020
	L-cysteine	1.32 to 1.40		13.1%	
MoS$_2$	SDS	110 to 230	100	19.07% to 19.71%	Raj et al., 2019
SiO$_2$	Linear alcohol	0.485	2.804	48.5% (total)	Kuang et al., 2018

*When the paper presents more than one RF, the table shows average values.

Although there are several recommendations for the formulation and selection of an NF, it is important to emphasize that there is no general formulation, as the RF depends on the type of reservoir and oil characteristics (Table 3.8).

Table 3.8. Relationship between the RF, NF, and oil properties

NP	Surfactant	Oil	ρ (g/cm³)	RF*	Reference
TiO$_2$	CTAB	Heavy crude oil	0.89	24% to 36%	Panahpoori et al., 2019
Fe$_3$O$_4$ covered with SLS	TW-80	Crude oil	0.90	20%	Shalbafana et al., 2019
Fe$_3$O$_4$ covered with EDTA				13.49%	
MoS$_2$	SDS	Crude oil	0.86	19.07% to 19.71%	Raj et al., 2019
Fe$_2$O$_3$	SDS	Crude oil	0.94	11%	Divandari et al., 2019
G-DSu	SDBS	Crude oil	0.833 g/L	8% to 14%	Radnia et al., 2018
Carbon nanotube	SDS	Crude oil	0.869	12.22% to 18.57%	Soleimani et al., 2018
SiO$_2$	Alkyl ammonium	n-Decane (Extra Dry. AcroSeal)	0.81	45% (total)	Kuang et al., 2018
	OA			41.5% (total)	
	PAA			45% (total)	
	Linear alcohol			48.5% (total)	

Al₂O₃	OA			40% (total)	
	PAA			44% (total)	
	Linear alcohol			47.5% (total)	
SiO₂	Linear alcohol ethoxylated	Crude oil	0.849	14.1% to 15.4%	Rognmo; Heldal; Ferno, 2018
SiO₂				10.1%	
SiO₂	KD	Crude oil	0.8503 mg/L	18.16% to 21.56%	Xua et al., 2019
SiO₂	T-100	Crude oil dehydrated mixed with kerosene	0.8232	16%	Zhao et al., 2018
SiO₂	L-arginine	Crude oil	0.875	12.7%	Asl et al., 2020
	L-cysteine			13.1%	
SiO₂	SDS	Crude oil	0.8399	59% to 78%	Mohajeri et al., 2019

3.6 CONCLUDING REMARKS

The selection of nanoparticles for application in nanofluids is of great importance in enhanced oil recovery, and several factors need to be considered for the optimization of the nanofluid formulation, such as compatibility of the physical and chemical nature of nanoparticles (metallic, non-metallic, magnetic, organic, or inorganic).

The size of the NP – although it must be nanometric – does not interfere much with the recovery factor in enhanced oil recovery processes using nanofluids. In addition, foam stabilization by adjusting the size of the NPs does not have a direct influence on the Recovery Factor (RF). The nanofluid interfacial tension should be below, although there is no consensus on this matter. Regarding wettability and contact angle, several studies report that the smallest contact angles do not result in high RF.

This review article points out that the viscosity of NF should be close to that of oil to achieve higher recovery factors, with viscosity being particularly dependent on the type and concentration of the surfactant and not modified by the size of the NP. The apparent properties of NF (viscosity, surface tension, wettability, etc.) depend on the interaction and adsorption of surfactant in NP. Research efforts should focus on the

importance of surfactant adsorption on different types of oil, as it was observed that NF that result from high surfactant adsorption on NP result in higher tertiary recovery factors.

4 A REVIEW ON THE SYNTHESIS AND APPLICATION OF NANOPARTICLES IN ENHANCED OIL RECOVERY

This chapter presents a theoretical background and literature review about the synthesis and characterization of nanoparticles applicable to the nanofluid formulation. Here, the main theoretical aspects related to the synthesis of nanoparticles and characterization of nanoparticles for application in Enhanced Oil Recovery (EOR) are presented.[2]

4.1 INTRODUCTION

Fossil fuels have been the world's main energy source since the nineteenth century and are expected to remain so for several decades to come (Nasr et al., 2021). World energy consumption is projected to increase by 50% by 2040 and, despite the increased attention and huge investments in renewable energy, energy demand is unlikely to be completely met by renewable sources alone by that time (Sun et al., 2020; Yakasai et al., 2021).

Since fossil fuels are non-renewable energy sources, mature oil fields are facing a phase of decline. It is estimated that 60% to 70% of the total oil remains in reservoirs when conventional hydrocarbon recovery techniques are employed (Kang et al., 2011). To overcome this drawback, efforts have been made to improve oil extraction from existing reservoirs using Enhanced Oil Recovery (EOR) techniques (Rezk and Allam, 2019a; Sun et al., 2020).

In this context, several studies have investigated the use of nanoparticles in EOR, some of which have demonstrated great success in overcoming the challenges of common EOR methods (Ali et al., 2020; Foroozesh and Kumar, 2020). When nanofluids are injected into reservoirs, nanoparticles are disposed of within the three-phase oil-water-rock system creating a film that serves as a wedge between the rock surface and the oil phase, exerting an excess pressure (disjoining pressure) which stimulates oil separation from the rock surface (Kondiparty et al., 2011). Nanofluids are used to improve oil recovery from different kinds of oil reservoirs due to their ability to modify some crucial parameters in porous media, such as wettability, and interfacial tension between water and oil, and to unlock oil trapped in the pore systems of reservoirs (Ali et al., 2018).

---

[2] This Chapter is part of a review paper entitled "An Overview on Synthesis Procedures of Nanoparticles Applied to Enhanced Oil Recovery", which is currently under review in *Petroleum Science and Technology*.

Several properties make nanoparticles potential materials for application in EOR, such as their small size, high surface area to volume ratio, thermal and mechanical stability, and high surface energy (Gbadamosi et al., 2018; Foroozesh and Kumar, 2020). It is known that the surface properties of nanomaterials can differ greatly depending on the synthesis method employed (Alomair et al., 2015). This provides an excellent value proposition for exploring the relation of nanoparticle synthesis methods to performance in enhancing oil recovery in reservoirs.

Therefore, this review article presents the synthesis methods most employed in the preparation of nanoparticles for EOR purposes. The influence of nanoparticle synthesis methods on contact angle and interfacial tension is discussed, as well as the efficiency of the nanofluids in enhancing oil recovery. The size and zeta potential of the nanoparticles are also highlighted. Finally, challenges and future perspectives in the application of nanoparticles to improve EOR techniques are presented.

4.2   KEY FEATURES OF NANOPARTICLES

The size of nanoparticles and their distribution in the base fluid play an important role in obtaining good performance from nanofluids (Shaw, 2020). Overall, research suggests that oil recovery increases with decreasing particle size, which is also observed for wettability alteration and reduction of interfacial tension (IFT) (Eltoum et al., 2021). Nanofluids usually remain stable when the suspended nanoparticles are small and do not agglomerate. Due to their small size, nanoparticles can easily circulate in porous media and are readily able to flow in narrow pores without getting trapped (Rezk and Allam, 2019a). However, depending on the size of the nanoparticle, they may block the pores, causing a so-called "mechanical entrapment", which occurs when the pore is smaller than the nanoparticle or when nanoparticles accumulate as the nanofluid move through the pores, narrowing the pores (Schneider, José, and Moreira, 2021). Simultaneously, nanoparticles are susceptible to aggregating to reduce surface energy, leading to a thermodynamic instability of colloidal dispersions (Sun et al., 2020).

Since the stability of nanofluids is a determining factor for good performance in oil recovery, several studies observed that the dispersion of nanoparticles in the base fluid can be enhanced by employing sonication or surfactant addition (Cheraghian et al., 2017; Tiwari et al., 2021). Sonication is a widely used technique that prevents aggregation by physically breaking large agglomerates to form well-dispersed nanofluids, while the

addition of surfactant coats the nanoparticles' surface and reduces the surface tension of the suspension, enhancing the dispersibility of nanoparticles (Shaw, 2020).

Zeta potential measurement is used to estimate the stability of a suspension by balancing van der Waals attraction forces and electrostatic repulsive forces (Yakasai et al., 2021). A high zeta potential (usually higher than 30 mV) indicates that nanoparticles repel each other and remain suspended in the nanofluid, characterizing a more stable suspension, while a low zeta potential (lower than 30 mV) is indicative of a high tendency of particles to agglomerate, showing less stability (Omar et al., 2014; Zainon and Azmi, 2021).

4.3   SYNTHESIS OF NANOPARTICLES

The preparation of nanoparticles can play an important role in controlling their physicochemical properties, influencing the stability of the nanofluid (Said et al., 2021). Several types of nanoparticles can be prepared to compose a nanofluid, such as metallic oxides, graphene, carbon nanotubes, and silica (Said et al., 2021). Examples of widely accepted preparation techniques for nanoparticles are hydrothermal, co-precipitation, sol-gel, chemical vapor deposition, biosynthesis, Stöber, and Pickering methods.

4.3.1   Hydrothermal method

In this technique, the solid precursors are mixed in water (distilled or deionized) and agitated until the solution is completely homogenized. Usually, if the solvent is different from water the process is called solvothermal synthesis. The method involves heating the reactants in a particular solvent in a high-pressure system such as an autoclave. The reaction takes place when the solution is transferred to the autoclave and is kept at high temperatures (150 to 300 ºC) for long periods (12 to 24 h). Table 4.1 presents examples of nanoparticles synthesized by hydrothermal and solvothermal methods applied to EOR.

Table 4.1. Nanoparticles applied to enhanced oil recovery synthesized by hydrothermal and solvothermal methods.

Nanoparticles	Base fluid	Size (nm)	Zeta potential (mV)	CA (degrees)		IFT (mN/m)		Reference
				Pure	With NP	Pure	With NP	
ZnO	Water/SDS	50	-	-	-	32.5	7.1	Rezk and Allam (2019b)
MoS$_2$	Brine	100	28	95	18	-	0.2	Raj et al. (2019)
Graphene	Water	3.5	-	-	-	16.8	0.9	Nasr et al. (2021)
ZrO$_2$	Brine/CTAB	100	-	-	75	-	8.4	Jha et al. (2021)
Fe$_2$O$_3$	Brine	175	5.01	32.4	75.5	49.1	26.4	Chen et al. (2021)
Faujasite	Brine	24	-	33	126	36	25	Taleb et al. (2021)

Raj et al. (2019) achieved a low surface tension and observed that the contact angle decreased with MoS_2 nanoparticles, confirming an alteration in the wettability from an intermediate-wet to a water-wet state. A water-wet system is defined as one with a contact angle between 0° and 75° for water droplets, a range from 75° to 120° reveals neutral wettability, and a range between 120° and 180° shows oil wettability of the system (Shalbafan et al., 2020). The zeta potential measure at the rock/water interface was found to be negative, while the nanofluid had a positive charge. Thus, MoS_2 was deposited over the surface, altering the wettability of the system to water-wet.

Nasr et al. (2021) reported that Graphene-quantum-dots nanofluids with a low size range (about 3.5 nm) led to a higher wettability alteration of carbonate rocks and decreased the oil/water IFT. Thus, the reduction in IFT becomes more pronounced because more nanoparticles can accumulate at the interface.

4.3.2   Co-precipitation

In this method, synthesis is carried out by mixing inorganic salts in an aqueous medium followed by precipitation with hydroxide. The precipitate is digested, filtered, and dried, usually at mild temperatures (50 to 80 °C). Examples of nanoparticles synthesized by the co-precipitation method and investigated for oil recovery can be found in Table 4.2.

Table 4.2. Nanoparticles applied to enhanced oil recovery synthesized with the co-precipitation method.

Nanoparticles	Base fluid	Size (nm)	Zeta potential (mV)	CA (degrees)		IFT (mN/m)		Reference
				Pure	With NP	Pure	With NP	
Fe_3O_4 - EDTA/SLS	Brine	20 -50	-54.2	140	22	-	-	Shalbafan et al. (2019)
Fe_3O_4 - Citrate	Brine	-	-30	160	114	11.2	7.9	Izadi et al. (2019)
Fe_3O_4 - PVP/SDS	Water	5 - 15	-	140	23	-	-	Shalbafan et al. (2020)
Fe_3O_4	CTAB	6	-	90	30	30	1	Pereira et al. (2020)
Fe_2O_3	Brine	37.9	-	-	-	40	36.8	Wahaab et al. (2020)
Polymer	Brine	23.1	-	115.8	51.3	16.2	0.08	Zhou et al. (2020)
$CaCO_3$	Water	55.4	-	116.4	28.7	-	-	Rashidi et al. (2021)

In the study performed by Shalbafan et al. (2019), Fe_3O_4 nanoparticles were prepared by co-precipitation and coated with EDTA or SLS. The functionalized nanoparticles completely altered the wettability of carbonate rocks from a strongly oil-wet to a strongly water-wet condition. Moreover, the nanofluids reached a zeta potential of approximately −50 mV, showing long-term stability and good dispersion.

Zhou et al. (2020) investigated a novel nanofluid that can tolerate harsh conditions, such as high temperature (≥80 °C) and high salinity (≥15%), to maintain the nanofluid stability. Thus, two hydrophobic polymers were used as precursors. The authors concluded that the nanocomposite remained stable because the surfactant itself has a strong chelation interaction with divalent metal ions and good salinity resistance. Moreover, the surfactant molecules adsorbed on the surface of the nanoparticles provided a strong steric repulsion which further stabilized the nanocomposite. Regarding the hydrophobicity and hydrophilicity of the nanomaterials applied in EOR, although there is no consensus about the use of hydrophilic materials, such as SiO_2 hydrophilic, these nanoparticles have a great potential for EOR, being up to 40% higher than hydrophobic SiO_2 nanoparticles (Rognmo, Heldal, and Ferno, 2018)."

4.3.3 Sol-gel

The sol-gel method is widely used to produce silica, glass, and ceramic materials under mild conditions, and it is known for its ability to control particle size, distribution, and morphology. The process usually consists of hydrolysis and condensation of metal lakesides in the presence of an acid or base (Negi et al., 2021). Thereby, the solution forms a two-phase system, containing two phases, liquid and solid. Examples of nanoparticles prepared by the sol-gel method and applied for EOR are presented in Table 4.3.

Table 4.3. . Nanoparticles applied to enhanced oil recovery synthesized by the sol-gel method.

Nanoparticles	Base fluid	Size (nm)	Zeta potential (mV)	CA (degrees)		IFT (mN/m)		Reference
				Pure	With NP	Pure	With NP	
Janus-SiO_2	Water	2.6	-39.8	-	10.9	30.2	17.2	Yin et al. (2019)
Al_2O_3	Brine/SDBS	109.4	-	56.4	18.7	22.3	7.7	Adil et al. (2020)
SiO_2	-	68	-	95	65	6	1.5	López et al. (2020)
Al_2O_3/SiO_2	CTAB	20 to 30	-	157	19	-	-	Rezvani et al. (2020)
MoS_2 QDs/N-doped GQDs	CTAB or SDBS	2 to 5	-	87.7	64.5	53.9	15.7	AfzaliTabar et al. (2020)
SiO_2	Brine or Water	14	-	150	23	25.1	9.3	Keykhosravi et al. (2021)

Adil et al. (2020) prepared nanoparticles of Al_2O_3 by the sol-gel method and used brine and SDBS to prepare the nanofluid. For smaller nanoparticles, the surface free energy changed in correspondence to the surface to volume ratio which resulted in a decline in CA and IFT measurements.

The study performed by Rezvani et al. (2020) investigated the application of Al_2O_3/SiO_2. With the addition of Al_2O_3/SiO_2 and CTAB, the contact angle decreased from 157° to 19°. In this case, the NPs arranged in the space between the oil and solid surface apply a disjoining pressure to the surface of the glass. The adsorption of NPs intensifies the disconnection pressure and results in the detachment of oil droplets from the surface.

4.3.4   Chemical vapor deposition

The method based on Chemical Vapor Deposition (CVD) is usually employed to produce solid materials with significant purity. In this method, a substrate is exposed to one or more volatile precursors, which react or decompose on the substrate surface, producing the desired deposit. Table 4.4 shows examples of nanoparticles produced by CVD, which are used for EOR applications.

According to Soleimani et al. (2018), CVD is a simple and economical technique for synthesizing carbon nanotubes. Radnia et al. (2018) prepared nanoparticles of graphene using CVD, carried out in an electrical furnace with a quartz reactor at 900-1100 °C for 5 to 30 min using methane as the carbon source and hydrogen as the carrier gas.

4.3.5   Biosynthesis

In the biosynthesis method, microorganisms can act directly in the intracellular or extracellular synthesis of metallic nanoparticles. Due to its green nature and eco-friendly steps, biosynthesis is considered a promising alternative in the field of materials technology. Table 4.5 presents details about nanoparticles prepared by the biosynthesis method for EOR applications.

Table 4.4. Nanoparticles applied to enhanced oil recovery synthesized by the chemical vapor deposition method.

Nanoparticles	Base fluid	Size (nm)	Zeta potential (mV)	CA (degrees)		IFT (mN/m)		Reference
				Pure	With NP	Pure	With NP	
Graphene	Water	-	-30	165	107	14.5	12.9	Radnia et al. (2018)
SiO_2-graphene	Brine	5	-	-	-	19.1	7.1	Tajik et al. (2018)
Carbon Nanotubes	Water/SDS	110	-	-	-	27	< 18	Soleimani et al. (2018)

Table 4.5. Nanoparticles applied to enhanced oil recovery synthesized by biosynthesis.

Nanoparticles	Base fluid	Size (nm)	Zeta potential (mV)	CA (degrees)		IFT (mN/m)		Reference
				v	With NP	Pure	With NP	
$ZnO/SiO_2/Xanthan$	Seawater	<100	-	91.6	34.1	31.8	2.2	Ali et al. (2019)
$TiO_2/Quartz$	Water or Seawater	3.5	-	103	48	36.4	3.5	Zargar et al. (2020)
SiO_2	Water	25	-	148	97	60	17.3	Zamani et al. (2020)
$Fe_3O_4/$ eggshell	Water/ CTAB or TR-880	20 to 35	-	-	62	-	0.2	Omidi et al. (2020)
$SiO_2@$ Montmorilant@Xanthan	Water	31 to 50	-32	150	33	35	15	Nazarahari et al. (2021)

4.3.6   Stöber and Pickering methods

The Stöber method is a chemical process used to prepare silica (SiO$_2$) nanoparticles of controllable and uniform size for applications in materials science. The method is based on the hydrolysis and condensation of alkyl silicates under alkaline conditions (Wang et al., 2010) and still is the most used wet chemistry synthetic approach to silica nanoparticles.

A Pickering emulsion is an emulsion that is stabilized by solid particles, such as colloidal silica, which adsorbs on the interface between two phases. This method is based on a particle-stabilized emulsion and is considered a versatile method for synthesizing a large quantity of Janus particles with control of the geometry and size (Jiang et al., 2010). A representation of this method is shown in Figure 4.2, where the authors used aminopropyldimethylethoxysilane (APS) to modify the silica particle surface. Table 4.6 shows reported studies where nanoparticles produced by the Stöber and the Pickering emulsion methods were used for EOR applications.

Figure 4.1. Synthetic route of SiO2 Janus nanoparticles. Reprinted from Jiang et al. (2010).
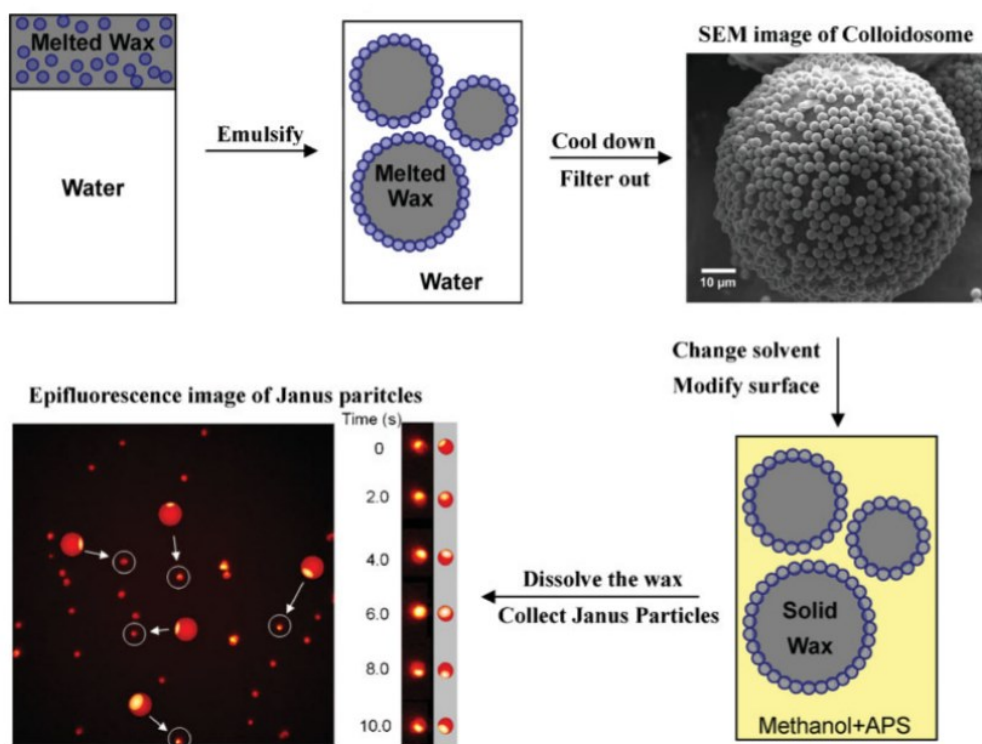
Table 4.6. Nanoparticles applied to enhanced oil recovery synthesized by the Stöber and the Pickering emulsion methods.

Nanoparticles	Method	Base fluid	Size (nm)	Zeta potential (mV)	CA (degrees)		IFT (mN/m)		Reference
					Clean	With NP	Clean	With NP	
SiO_2	Stöber	PAM and ethanol	34 to 39	-35	-	-	-	-	Chaturvedi and Sharma (2021)
SiO_2	Stöber	-	40	-	-	-	-	-	Liu et al. (2017)
NiO/SiO_2 Janus	Stöber	-	58	-40	41	19	26.2	17	Giraldo et al. (2019)
SiO_2 Janus	Pickering	Brine	40	-	121.4	63	30	2.3	Wu et al. (2020)
SiO_2 Janus	Pickering	-	-	28.1	-	47.9	-	-	Jia et al. (2021)

4.4   PERFORMANCE OF NANOPARTICLES IN EOR

Table 4.7 presents the results in terms of enhancing oil recovery efficiency obtained in the studies discussed earlier in this review.

Table 4.7. Percentage of enhanced oil recovery (EOR) using nanoparticles.

Nanoparticle	Method	Oil	EOR	Reference
SiO_2	Sol-gel	Degassed crude oil	33%	Keykhosravi et al. (2021)
SiO_2	Stöber	Oil (Tarapur Oilfield)	27%	Chaturvedi and Sharma (2021)
SiO_2	Sol-gel	Heavy crude oil	3%	López et al. (2020)
SiO_2	Biosynthesis	Crude oil	25%	Zamani et al. (2020)
SiO_2	Stöber	Light crude oil	21%	Liu et al. (2017)
SiO_2	Sol-gel	Heavy crude oil	16%	Taborda et al. (2016)
Silica Janus	Pickering emulsion	Crude oil	27.2%	Jia et al. (2021)
Silica Janus	Pickering emulsion	Crude oil	15.74%	Wu et al. (2020)
Silica Janus	Stöber	Light crude oil	6%	Giraldo et al. (2019)
Silica Janus	Sol-gel	Crude oil	18.31%	Yin et al. (2019)
Fe_3O_4	Co-precipitation	Crude oil	24.81%	Shalbafan et al. (2020)
Fe_2O_3	Co-precipitation	Crude oil	15.8%	Wahaab et al. (2020)
Fe_3O_4	Biosynthesis	Crude oil	8.16%	Omidi et al. (2020)
Fe_3O_4	Co-precipitation	Crude oil	18.1%	Izadi et al. (2019)

Fe$_3$O$_4$	Co-precipitation	Crude oil	20%	Shalbafan et al. (2019)
Graphene	Hydrothermal	Crude oil	18%	Nasr et al. (2021)
Carbon quantum dots	Hydrothermal	Crude oil	17%	Baragau et al. (2021)
MoS$_2$ QDs/N-doped GQDs	Sol-gel	n-decane	22%	AfzaliTabar et al. (2020)
Graphene	Chemical vapor deposition	Crude oil	19%	Radnia et al. (2018)
Carbon nanotubes	Chemical vapor deposition	Crude oil	18.5%	Soleimani et al. (2018)
CaCO$_3$	Co-precipitation	Crude oil	20%	Rashidi et al. (2021)
Faujasite	Hydrothermal	Crude oil	9.6%	Taleb et al. (2021)
SiO$_2$@ Montmorilant@ Xanthan	Biosynthesis	Crude oil	15.8%	Nazarahari et al. (2021)
ZnO	Sol-gel	Crude oil	13.1%	Adil et al. (2020)
Al$_2$O$_3$/SiO$_2$	Sol-gel	Heavy dead crude oil	73%	Rezvani et al. (2020)
Polymer	Co-precipitation	Crude oil	9.3%	Zhou et al. (2020)
TiO$_2$/Quartz	Biosynthesis	Crude oil	21%	Zargar et al. (2020)
MoS$_2$	Hydrothermal	Crude oil	21.2%	Raj et al. (2019)
ZnO	Solvothermal	n-dodecane	8%	Rezk and Allam (2019b)
ZnO/SiO$_2$/ Xanthan	Biosynthesis	Crude oil	19.3%	Ali et al. (2019)
SiO$_2$-graphene	Chemical vapor deposition	Crude oil	52%	Tajik et al. (2018)

SiO$_2$ is often applied to oil recovery and has also presented the best results when prepared by sol-gel or chemical vapor deposition, with a size between 5 and 30 nm. The characteristics of nanofluid are particularly important. Keykhosravi et al. (2021) synthesized silica nanoparticles by the sol-gel method and prepared nanofluids by dispersing the

nanoparticles in distilled water with an ultrasonic probe, with degassed crude oil, resulting in an oil recovery of 78% of original oil in place (OOIP), while 49% of OOIP were achieved with the injection of a slug nanofluid and continuous nanofluid flooding. These results led to an improvement in oil recovery efficiency of almost 30%.

The study performed by Rezvani et al. (2020) presented exciting results using Al_2O_3/SiO_2, reaching an oil recovery of 92% OOIP. In this study, the recovery factor of the conventional gas flooding was approximately 19% OOIP. The oil recovery improved with foam injections (with or without NPs) due to the higher viscosity of the foam. Moreover, the oil/water IFT was reduced by the presence of the surfactant in the foam, which increases the efficiency of oil displacement. With the injection of CTAB foam, the oil recovery increased to 50%, while with Al_2O_3/SiO_2 CTAB foam the oil recovery reached 92%, revealing an EOR of up to 73%, the oil used in this study was a havy dead crude oil.

Other expressive EOR result was observed in the study performed by Tajik et al. (2018). The authors synthesized SiO_2-graphene nanoparticles with the chemical vapor deposition method and functionalized them with a mixture of nitric and sulfuric acid vapors. The results showed that only 31% of oil can be recovered by water flooding, while 83% of the crude oil recovered was achieved when using the SiO_2-graphene nanofluid, representing an EOR of 52%.

4.5   CONCLUSIONS AND PERSPECTIVES

A review of the literature of the past 5 years made clear that the application of nanoparticles for EOR has attracted strong research interest and contributed to many experimental investigations. Nanoparticles produced by different synthesis methods have been characterized in terms of size, stability, interfacial tension, contact angle, and EOR measurements. The injection of nanofluids in rock reservoirs has shown great ability to change CA and IFT, which strongly influence the efficiency of oil recovery. As one of the main parameters, it is important to determine the IFT between oil/water, oil/brine, or oil/injected fluids to estimate the distribution and movement of fluids in porous media. In parallel, the reduction in CA and the wettability alteration from an oil-wet system to a water-wet one have a significant role in increasing oil production. Overall, all nanoparticles showed an

improvement in oil recovery, but their applications are mainly limited to laboratory scale, and it requires further research to prove their potential for field-scale implementation.

5 SYNTHESIS AND CHARACTERIZATION OF SILICA-BASED NANOFLUIDS FOR ENHANCED OIL RECOVERY

This Chapter describes the synthesis, characterization, and application of different sources of silica nanoparticles to produce nanofluids for enhanced oil recovery. The evaluation of enhanced oil recovery is also presented.[3]

5.1 INTRODUCTION

Nanotechnology is the area of science devoted to understanding the fundamental physics, chemistry, biology, and the technology of materials at the nanoscale (Ali et al., 2018). Because of this characteristic, nanotechnology has applications in different knowledge areas, like engineering, chemistry, physics, biology, medicine, among others.

Nanoparticles can be dispersed in fluid bases, like ethylene glycol, oil, water, brine, surfactants, etc., to prepare nanofluids (Maaref et al., 2020; Hou et al., 2022; Sircar et al., 2022). Depending on the nanoparticle characteristics and the fluid base, the stability, and the thermal, optical, electrical, rheological and magnetic properties can be adjusted for different applications (Awais et al., 2021; Suleimanov et al., 2011). In the petroleum industry, nanoparticles have been applied in drilling operations, wastewater treatment, corrosion inhibition, production, development, heat transfer, and enhanced oil recovery (Ali et al., 2020; Ali et al., 2020a; Abang et al., 2021; Mittal, 2022).

Oil recovery occurs in three steps: primary, secondary and tertiary recovery; the latter is also known as enhanced oil recovery (EOR). In primary recovery, the natural energy present in the reservoir is utilized, although only about 5-10% of the oil present in the reservoir is recovered. Water and gas are injected into the reservoir for the secondary recovery, and the oil recovery is 10-55%. Thus, after the primary and secondary recovery, a large amount of oil remains in the pores of the reservoir, due to the high capillary pressure of the water. Considering the large amount of oil that can still be extracted from a reservoir, tertiary recovery techniques

---

[3] Part of this Chapter intitled "Synthesis and Characterization of Silica-Based Nanofluids for Enhanced Oil Recovery" will be submitted to the Special Issue of Nanomaterials ("Synthesis and Application of Silicon Dioxide"). https://www.mdpi.com/journal/nanomaterials/special_issues

are applicable. To increase efficiency, biological, physical, and chemical methods are applied. In those cases, the ratio of mobility of the injected fluids is reduced, decreasing the interfacial surface tension between the fluid injected and the oil, reducing capillary forces and changing the wettability of the reservoir (Vishnyakov et al., 2020). EOR, allows an additional 5-15% of the oil from the reservoir to be recovered (Viswanathan, 2016).

In the chemical method, the association between nanoparticles and surfactants to prepare nanofluids for applications in EOR has been proposed by several authors in recent years (Agi et al., 2020; Ali et al., 2020; Ali et al., 2020a; Schneider et al., 2021; Lau et al., 2017; Behera et al., 2022; Mittal, 2022; Sircar et al., 2022). According to Mittal (2022), the application of nanomaterials has the potential to achieve outstanding results in the oil industry.

Surfactants are applied to reduce the surface tension between oil and water, facilitating the displacement of oil throughout the production pool, and–can be added to nanofluids to improve their characteristics and properties. Although the studies related to the application of nanofluids in enhanced oil recovery are relatively recent, their utilization can improve the economy of mature fields, because nanofluids can change the wettability of the rock surface, reduce interfacial tension and the viscosity of the oil phase (Suleimanov et al., 2011).

Numerous studies have reported the use of nanoparticles of silica (SiO_2), titanium dioxide (TiO_2), graphene oxide (GO), and aluminum oxide (Al_2O_3) to improve the rheology, and viscoelastic properties of nanofluids (Sircar et al., 2022). The preparation method of nanoparticles can play a key role in controlling their physicochemical properties, such as size, morphology, and zeta potential, influencing the stability of nanofluid (Said et al., 2021). Some examples of widely accepted preparation methods for nanoparticle synthesis are hydrothermal (Raj et al., 2019), co-precipitation (Shalbafan et al., 2019), sol-gel (Negi et al., 2021), chemical vapor deposition (Awais et al., 2018), and biosynthesis (Zamani et al., 2021). Other less common methods are also applied, such as milling (Agi et al., 2020), and the Stöber process (Wang et al., 2010).

Silica nanoparticles are extensively used in enhanced oil recovery because they can be easily adjusted to have the desired characteristics (Zulfiqar et al., 2016; Mittal, 2022). Nevertheless, the EOR mechanism of nanoparticles is extremely complex and includes several aspects such as wettability, injection fluid viscosity, surface tension alterations, and separation pressure (Idogun et al., 2016). Despite extensive investigation on SiO_2 nanoparticles for EOR

application, there are still challenges in the field owing to cost and huge environmental problems.

Recently, Agi et al. (2022) reported the application of silica nanoparticles from rice husks for chemical enhanced oil recovery and concluded that rice husk ash is a promising and cost-effective source to produce silica nanoparticles. However, deeper studies are required to formulate nanofluids to avoid nanoparticle agglomeration and increase oil recovery by adjusting operational conditions such as the nanoparticles concentration and nanofluid composition. Thus, this study aims to compare the efficiency of silica produced from rice husk ash and other silica-based nanofluids in the enhanced oil recovery process and to evaluate the effect of silica nanoparticle's characteristics and their concentration in the tertiary oil recovery.

5.2   EXPERIMENTAL

5.2.1   Materials

Sodium dodecyl sulfate (SDS, purity 96.44%, Neon), sodium silicate ($(Na_2O)x \cdot (SiO_2)y$) (3.3:1), 40-50 wt% in water, Quimidrol), aqueous ammonia (analytical grade, Biotech), and sodium chloride (NaCl, 99% purity, Vetec) were used without prior treatment or purification. Mineral oil (MO) SAE 90 GL-5 with a density of 0.90 g cm^{-3} was applied in the flooding tests since it presents comparable properties with petroleum from Campos Basin (Brazil) (Rangel et al., 2012). Moreover, the use of this oil in laboratory-scale tests has advantages such as easy cleaning procedures.

Three different silica nanoparticles were used in the nanofluid formulation. Commercial silica nanoparticles (SC) with a hydrophobic characteristic were purchased (Sigma-Aldrich). Two other samples were synthesized in this study from rice husk (Fumacence Foods, Santa Catarina, Brazil) or neutral sodium silicate as precursors.

5.2.2   Synthesis of nanosilica from rice husk

The methodology for synthesizing silica from rice husk ash (RH) was adapted from Agi et al. (2020). To remove organic matter, the rice husks were calcined at 800 °C for 7 h in a

muffle oven (F2-DM, Fornitec). Then, the material was washed with distilled water, filtered using a vacuum pump (820, Fisatom), and dried in an oven (DeLeo) at 100 °C for 15h. Finally, to obtain the particles on a nanometric scale, two consecutive milling steps were applied. The first milling step was conducted in a ball mill (CT 242, Servitech), for 4 h. Then, the material was milled in a micro-processed digital jar mill (CE-500/D, Cienlab), with a controlled velocity of 300 rpm for 5 h. Finally, the material was dried in an oven at 80 °C for 24 h.

5.2.3   Synthesis of nanosilica by sol-gel

The procedure for obtaining silica nanoparticles using the sol-gel method was based on Maaref et al. (2020); Chaturvedi, Sharma (2021); and Zulfiqar et al. (2016). First, 100 mL of sodium silicate were added to a beaker and kept in an ultrasonic bath (USC-1650A, Unique) for 15 min. Then, 60 mL of aqueous ammonia were added dropwise and kept in an ultrasound bath for 1 h, followed by a standing time of 20 min. Then, 200 mL of distilled water were added, and the solution was left to stand for 1 h. The precipitated solid was filtered and exhaustively washed with ethanol and distilled water to remove the ammonia residues to obtain silica by the sol-gel method (SS silica). Finally, the silica produced was dried in an oven at 250°C for 30 h.

5.2.4   Nanoparticle characterization

The synthesized, precipitated, and commercial silica were analyzed by X-Ray Fluorescence (XRF, Thermo Fisher), to determine the chemical composition of nanoparticles. The crystalline structure of the samples was evaluated by X-Ray Diffraction (XRD, MiniFlex600, Rigaku), at a scanning speed of $10°$ min^{-1} with a step size of $0.05°$.

A Transmission Electron Microscope (TEM, JEM 1011, JEOL) was used to analyze the inner structure of the samples, like the crystal structure, morphology, and stress state information. . Magnifications of 5000× to 300,000× were applied, with point and line image resolution of 0.23 nm and 0.14 nm, respectively, and a goniometric stage with a dual tilt module of ± 30º.

Fourier-Transform Infrared Spectroscopy (FTIR, Cary 660, Agilent) was used to identify the functional groups present on the surface of the samples. Dry nanoparticles were added to potassium bromide (KBr) before it was placed in a sample bearer.

The surface chemistry of the nanoparticles was determined by X-Ray Photoelectron Spectroscopy (XPS), using a PHI Versa-Pro II spectrometer utilizing a monochromatic Al Kα source (hν = 1486.6 eV, 150 W) and the pressure in the analysis during data acquisition was sustained below 1×10^{-9} Torr. The binding energy (BE) scale was corrected utilizing the position of the peaks for the C 1s (284.8 eV) of the adventitious carbon. The powder samples were mounted on a holder utilizing double-sided adhesive tape. Narrow spectral regions were recorded in addition to the survey photoelectron spectra. The pass energy during the analysis was 25 eV for the narrow scans and 160 eV for the survey spectra. The individual spectral regions were analyzed to calculate the relative ratios of the surface of the solid, identify the chemical state of the elements and determine the BE of the peaks. The obtained spectra were analyzed after applying Shirley's background subtraction and Gaussian (30%) – Lorentzian (70%) decomposition parameters using the Multipak software.

The analysis of the surface area and the pore size distribution were conducted using an gas sorption analyzer (Autosorb, Quantachrome) with Brunauer–Emmett–Teller (BET) and Barrett–Joyner–Halenda (BJH) methods, respectively. The N_2 adsorption-desorption isotherms measurement at 196 ºC was performed after degassing at 300 ºC for 24 h.

5.2.5 Nanofluid preparation

For the preparation of nanofluids, commercial silica nanoparticles (CS), rice husk ash derived silica (RH), and silica synthesized by the sol-gel method (SG) were used in a similar formulation, as displayed in Table 6.1. For the enhanced oil recovery tests, 14 different formulations were used: brine (B), brine with surfactant (BS), and 12 nanofluids (NF) prepared with brine, surfactant, and different concentrations of nanoparticles (Table 6.1).

Table 5.1. The concentration of silica nanoparticles, salt, and surfactant on solutions.

Silica nanoparticles	Fluid formulations	Concentration (wt%)		
		NaCl	Nanoparticle	SDS
-	Brine (B)	3.00	0.00	0.00
-	Brine + surfactant (BS)	3.00	0.00	0.12

	CS-NF0.10	3.00	0.10	0.12
Commercial-Silica (CS)	CS-NF0.25	3.00	0.25	0.12
	CS-NF0.50	3.00	0.50	0.12
	CS-NF0.75	3.00	0.75	0.12
	RH-NF0.10	3.00	0.10	0.12
Rice Husk-Silica (RH)	RH-NF0.25	3.00	0.25	0.12
	RH-NF0.50	3.00	0.50	0.12
	RH-NF0.75	3.00	0.75	0.12
	SG-NF0.10	3.00	0.10	0.12
Sol-gel Silica (SG)	SG-NF0.25	3.00	0.25	0.12
	SG-NF0.50	3.00	0.50	0.12
	SG-NF0.75	3.00	0.75	0.12

The brine was prepared by adding NaCl to distilled water; then, the solution was kept under magnetic stirring (MQAMA 301, Microquímica) for 10 min. For the BS solution containing surfactant, SDS was initially added to distilled water and the solution was kept under magnetic stirring for 30 min. Then, NaCl was added, and the solution was kept under stirring for another 10 min. The same procedure used for preparing BS was made for the nanofluids. However, after the second agitation, the percentage of nanoparticles was added to the solution (according to Table 6.1), and the solution was kept under magnetic stirring for 30 min. After that, the nanofluids were sonicated for 1 h (USC-1650A, Unique).

5.2.6 Nanofluid characterization

A particle size analyzer (Zetasizer Nano Series ZS, Malvern) was utilized to measure the particle size and zeta potential by Dynamic Light Scattering (DLS). The procedure was made at 25 °C and the powder samples were dispersed in distilled water (0.1 wt%) using an ultrasound bath for 1 h. To measure the size and zeta potential of the particles in the presence

of NaCl and surfactant, components present in nanofluids, the samples were prepared with a concentration of 0.75 wt% nanoparticles, 3.0 wt% sodium chloride, and 0.12 wt% surfactant.

The relative viscosity of nanofluids was analyzed in the function of the shear rate using a rotatory rheometer (Haake Mars, Thermo). The following parameters were selected for the analysis: geometry with a diameter of 60 mm; shear rate from 0 to 50 s^{-1}, gap of 150 μm, and room temperature.

The turbidity of nanofluids was measured six times (before the sonicator bath; 1 h, 2 h, and 24 h after the bath; and the last was after the flooding tests) using a turbidimeter properly calibrated with a 0.1 to 1000 NTU pattern scale. The relative viscosity of nanofluids was analyzed in the function of the shear rate using the samerheometer (Haake Mars, Thermo). The following parameters were selected for the analysis: plate-plate, geometry with a diameter of 60 mm; shear rate from 0 to 50 s-1, gap of 150 μm, and room temperature.

Finally, the Interfacial Tension (IFT) of nanofluids was measured using a goniometer (250, Ramé-Hart). In these analyses, 3 μL drops of fluids (oil, water, solutions, or nanofluids) at room temperature were deposited over a clean borosilicate glass surface. Measurements of surface tension were performed in triplicate and the results were determined by the mean of the values obtained.

5.2.7 Oil recovery tests

The experimental apparatus used in the oil recovery tests is shown in Figure 6.1. A fixed-bed column (7.5 cm in diameter and 35.5 cm in height) with ascending flow was employed to simulate an oil reservoir, as proposed by Son et al. (2014) and Rangel et al. (2012). The column bed, prepared before starting each recovery test, was comprised of a mixture containing 950 mL of mineral oil and 1.058 kg of sand (950 mL).

The sand used as a porous medium was purchased from a local market (Santa Catarina, Brazil). It was sieved to obtain a size between 300 and 600 μm and then washed for 3 h with distilled water according to the same experimental system as the flooding tests. Subsequently, the sand was dried in an oven (DeLeo) at 80 °C for 24 h.

Oil recovery was initially performed using 4 L of saline solution (B) injected into the system for 5 h using a rotary pump (75211-15, Cole-Parmer). Afterward, the enhanced recovery

of residual oil from the bed begins by feeding 4 L of the BS solution for 5 h (flow rate: 0.8 L h^{-1}), followed by feeding 4 L of nanofluid through the column (0.8 L h^{-1}). At this stage, a certain amount of oil is recovered, and another amount remains in the reservoir. The amount of oil recovered was measured in a graduated cylinder (Figure 6.1-V), for the B, BS, and each nanofluids samples, and the amount of oil recovered is expressed as a percentage (wt%). The mixture of oil and water collected from the porous cell was kept at rest for 24 h and then the fluids are separated, using a density separator, and each volume is measured (Rangel et al., 2012).
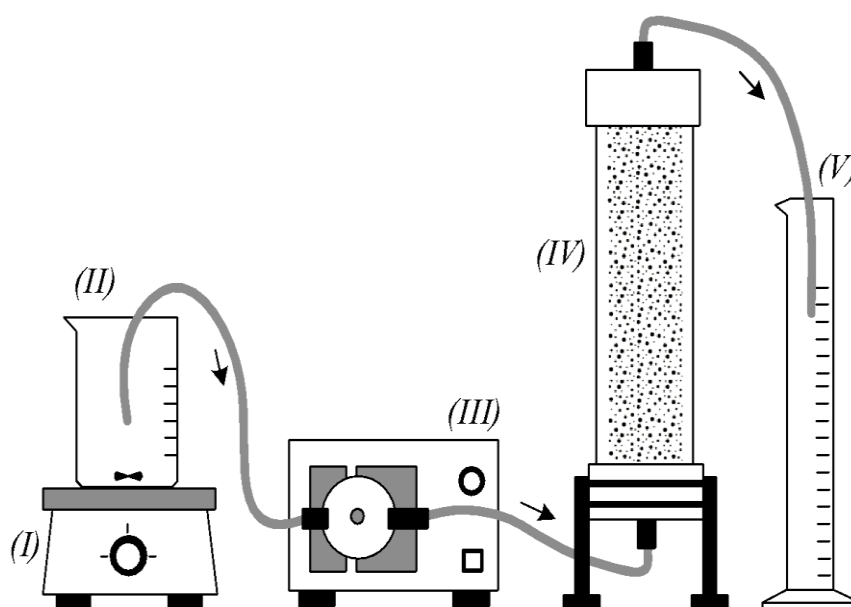
Figure 5.1. Experimental scheme of the system for oil recovery tests: (I) magnetic stirrer; (II) fluid reservoir; (III) rotary pump; (IV) fixed-bed column and (V) graduated cylinder.

5.3   RESULTS AND DISCUSSION

5.3.1   Characterization of silica nanoparticles

The chemical compositions of particles are shown in Table 6.2, as determined by XRF. The silica obtained from rice husk (RH) presented the highest purity among the three samples with 94.01 ± 0.26 wt% of SiO$_2$ and about 5.99 wt% of impurity that includes K, Ca, P, Mg, Al, Mn, Fe, Zn, S, Zr, and Ti.

Table 5.2. Chemical composition by X-ray fluorescence of commercial nanosilica, RH silica, and SG silica.

	Commercial silica (wt%)	RH silica (wt%)	SG silica (wt%)
SiO$_2$	89.87 ± 0.33	94.01 ± 0.26	69.29 ± 0.51
K$_2$O	0.0386 ± 0.0017	1.33 ± 0.05	0.0428 ± 0.0019
CaO	0.0109 ± 0.0010	0.833 ± 0.08	0.0127 ± 0.0012
P$_2$O$_5$	-	0.515 ± 0.017	-
MgO	-	0.439 ± 0.049	-
Al$_2$O$_3$	1.07 ± 0.09	0.273 ± 0.024	0.112 ± 0.0098
MnO	-	0.219 ± 0.0083	-
Fe$_2$O$_3$	0.117 ± 0.0095	0.183 ± 0.015	0.0747 ± 0.0060
ZnO	-	0.0434 ± 0.0009	-
SO$_3$	0.0356 ± 0.0022	0.0180 ± 0.0011	-
ZrO$_2$	0.0165 ± 0.0021	0.0112 ± 0.0008	0.0363 ± 0.0019
TiO$_2$	0.0452 ± 0.0010	0.0108 ± 0.0007	0.0857 ± 0.0014
Na$_2$O	0.941 ± 0.05	-	26.79 ± 0.24
Loss on ignition	7.83	2.09	0.56

The crystalline structure of all silica nanoparticles was evaluated by XRD (Figure 6.2). The commercial and sol-gel silica nanoparticles are amorphous materials, and a broad signal can be observed at about 2θ = 23° corresponding to the (002) reflection of amorphous silica in CS and SS silica (Guerrero et al., 2008). As previously reported by Zulfiqar et al. (2016), the synthesis of silica nanoparticles from sodium silicate under alkaline conditions produces only amorphous nanoparticles.

On the other hand, RH silica is crystalline and shows a dominant peak in the XRD pattern at 22° due to the presence of crystalline SiO$_2$ in RH. The sharp narrow peaks at 22, 26, 31 and 36° are attributed to cristobalite, tridymite, and quartz as polymorphs of crystalline silica that were formed due to the high temperature-time treatment of rice husk (800 °C, 7 h) (Steven et al., 2021). With the help of relevant equations and XRD results, the crystallite size of RH can be estimated as 27 nm.
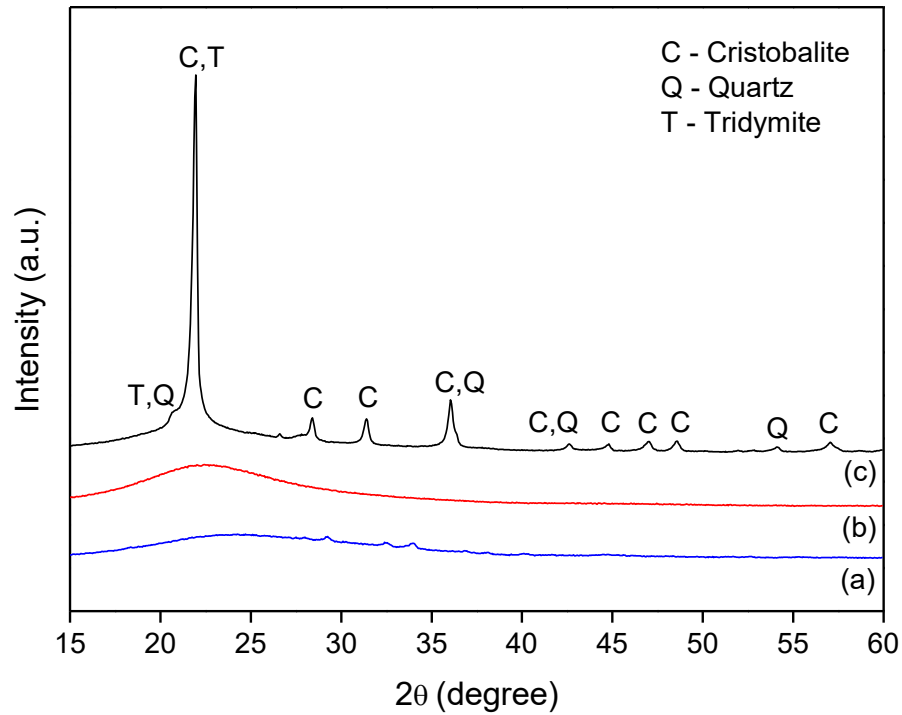
Figure 5.2. XRD diffractograms of SG (a), CS (b) and RH (c) samples.

TEM was used to determine the geometry and shape of the nanoparticles (Figure 6.3). The images reveal a spheroidal structure of the nanoparticles, and their respective size of ~27 nm, ~44 nm, and 2453.0 nm for CS, RH, and SG nanoparticles. The diffraction patterns obtained by TEM (Figures 6.3C, 6.3F, and 6.3I) confirmed that the commercial and SG silica particles are in an amorphous phase, while RH silica presents crystallinity.
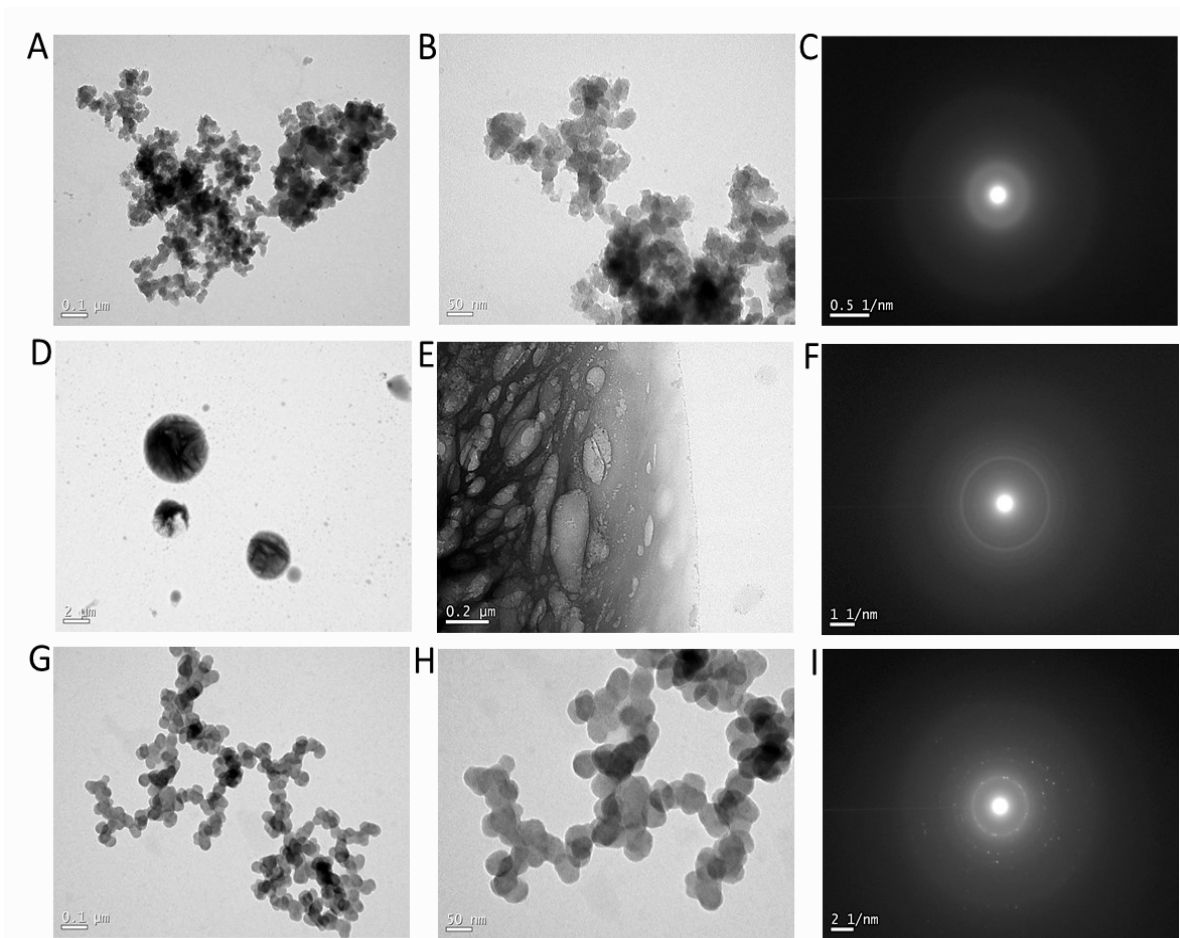
Figure 5.3. TEM analysis of the samples: A) CS structure in 100.000×; B) CS structure in 300.000×; C) CS diffraction pattern; D) SG structure in 5.000×; E) SG structure in 50.000×; F) SG diffraction pattern; G) RH structure in 100.000×; H) RH structure in 300.000; I) RH diffraction pattern

The textural characterization of silica nanoparticles is shown in Table 6.3. Low BET surface area and pore volume were measured for RH and SG nanoparticles while CS is a mesoporous solid (Figure 6.4).

Table 5.3. Characteristics of silica samples

Samples	Specific surface area (m² g⁻¹)	Average pore size (Å)	Pore volume (cm³ g⁻¹)
CS	99.6	317.5	0.793
RH	8.8	252.6	0.056
SG	1.1	216.8	0.003
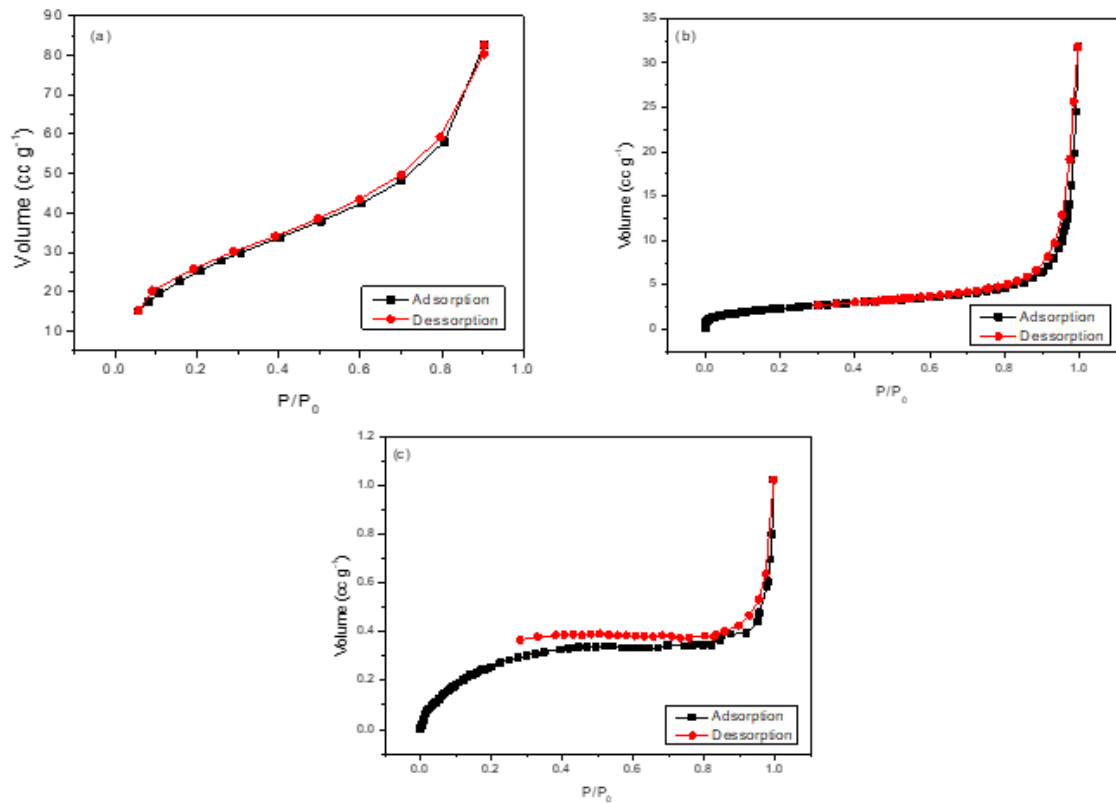
Figure 5.4. N2 adsorption-desorption isotherms of the CS (a), SG (b), and RH silica (c).

The FTIR spectra of the silica nanoparticles are shown in Figure 6.5. The peaks at 3436 and 953 cm^{-1} can be attributed to the O-H groups of the stretching vibrations present in the silanol hydroxyl groups (Si-OH). The deformation of water molecules absorbed on the SiO_2 surface appears at 1635 cm^{-1}. The peaks at 2920 and 2856 cm^{-1} are associated with antisymmetric elongation and elongation in -CH_2 groups, respectively. The peaks at 1225; 1105; 804; 619 and 484 cm^{-1} are characteristic of silica and can be related to different modes of Si–O vibration (Agi et al., 2020; Tian et al., 2017; Athinarayanan et al., 2015).
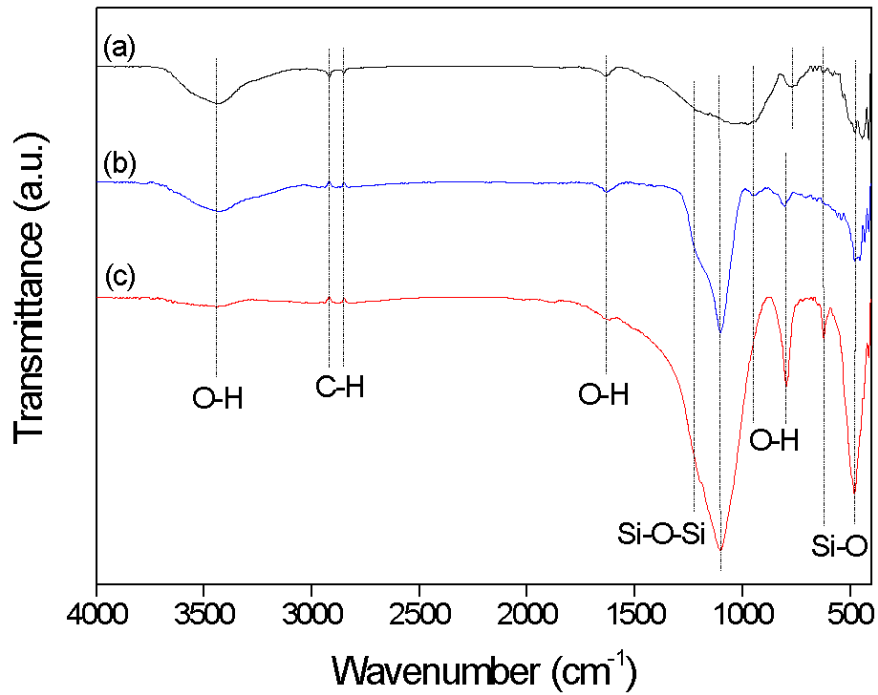
Figure 5.5. FTIR absorbance spectra of the SG (a), CS (b), and RH silica (c).

The FTIR spectra confirm the existence of Si and O. In addition, they did not show the significant presence of organic and inorganic materials, which confirms the high purity observed for the RH and commercial samples in the XRF analysis.

XPS analysis (Figure 6.6) was performed to obtain the composition and chemical states of the silica particles' surface, and the results are presented in Table 6.4. The XPS decomposed atom electron orbitals spectra are illustrated in Figures 6.7, 6.8, and 6.9 for commercial silica, RH silica, and SG silica, respectively.
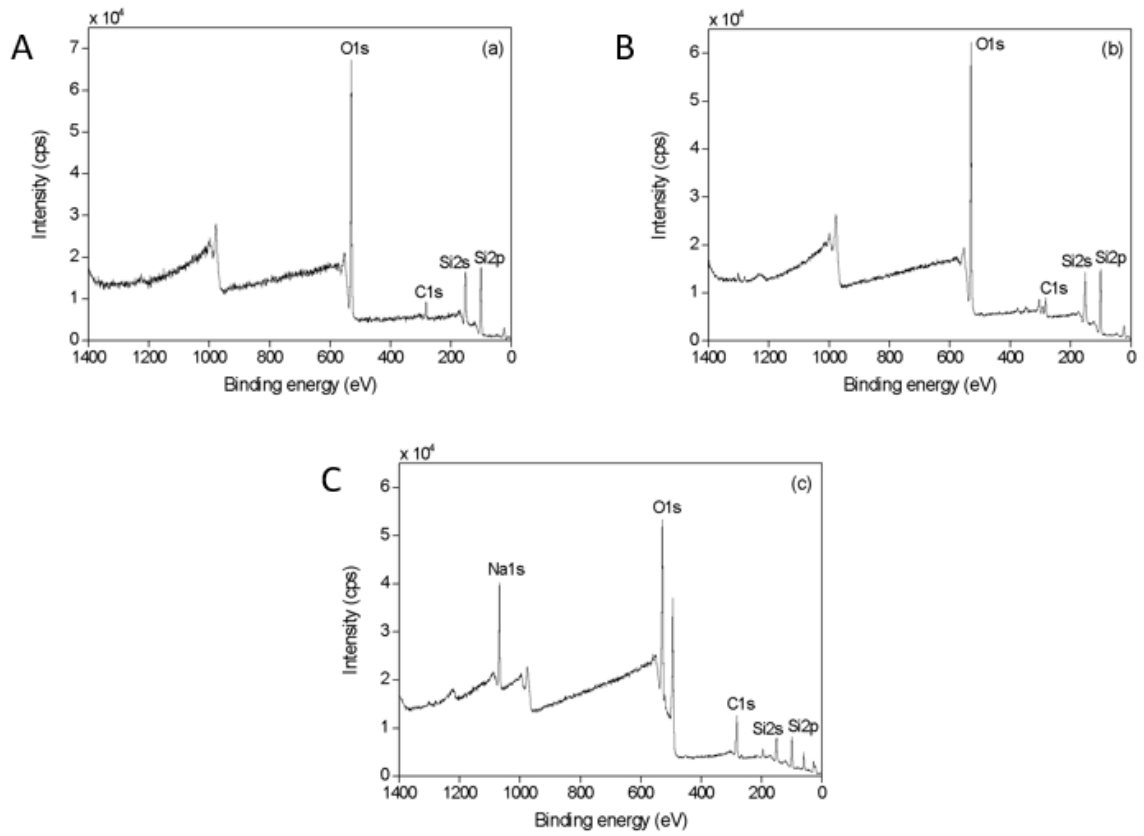
Figure 5.6. XPS spectra for silica nanoparticles: A) commercial; B) RH; and C) SG.

Table 5.4. XPS analysis and quantification for commercial, RH, and SG silica.

Element		Composition (At%)		
		Commercial SiO$_2$	RH SiO$_2$	SG SiO$_2$
Elemental analysis, At%	C	12.0	18.3	23.7
	O	59.4	57.1	48.0
	Na	0.6	0.2	15.2
	Si	30.0	21.9	11.9
	Mg	-	1.3	-
	K	-	1.2	-
	Cl	-	-	1.2
C1s	-	284.8 eV (84.5 %)	284.9 eV (100%)	284.9 eV (78.5%)
	-	285.8 eV (15.5%)	-	289.3 eV (21.5%)
O1s	-	-	-	531.0 eV (27.1%)
	-	533.0 (100%)	532.7 eV (100%)	532.5 eV (61.9%)
	-	-	-	536.0 eV (11.0%)
Na1s	-	1072.7 eV (100%)	1071.5 eV (100%)	1071.6 eV (100%)
Si2p	-	103.5 eV (100%)	103.5 eV (100%)	103.1 eV (100%)

The carbon spectra were compensated concerning the adventitious carbon contamination (Figures 6.7, 6.8, and 6.9). Subsequently, the C1s spectra were deconvoluted into peaks that corresponded to the hydrocarbon (C–C) at 284.8 eV (commercial silica) or 284.9 eV (RH and SG silica); ethoxy (C–O) at 285.8 eV (commercial silica), and carbonyl (C=O) at 289.3 eV (SG silica) (Wang et al., 2017; Davydov et al., 2014; Dolgov et al., 2015). The C–O chemical bonds could be C–O–C or C–O–H while the C=O group can be assigned to the COOH

or HO–C–OH bonds (Davydov et al., 2014). It can be seen that the -CH$_2$- was presented on the surface of all SiO$_2$ nanoparticles, which was in good agreement with the FTIR analysis. The Si2p spectra of the silica samples all showed a main peak at ~103 eV which corresponds to Si–O bonds demonstrating the existence of pure SiO$_2$ (Arunmetha et al., 2015; Bakdash et al., 2020; Zhang et al., 2016). Sodium (Na1s) are present in all surface samples at ~1071-1072 eV (Montes et al., 2020), especially in SG nanosilica, as also measured by XRF.
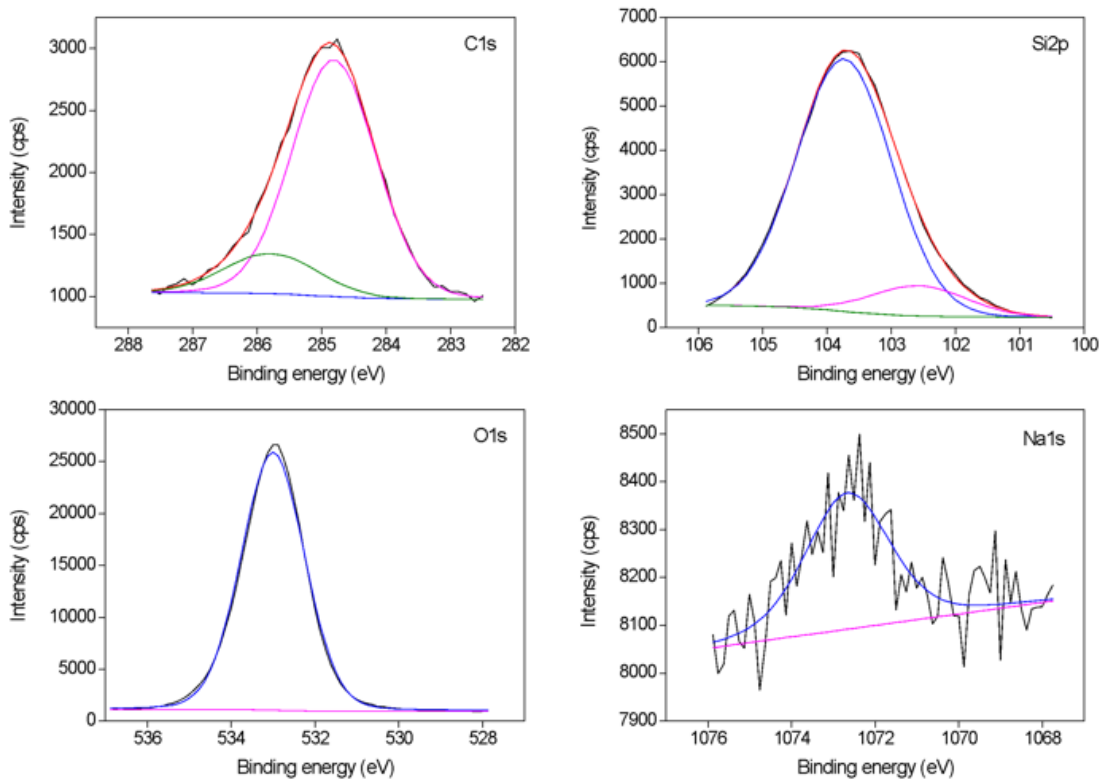
Figure 5.7. XPS decomposed atom electron high-resolution spectra for commercial silica.
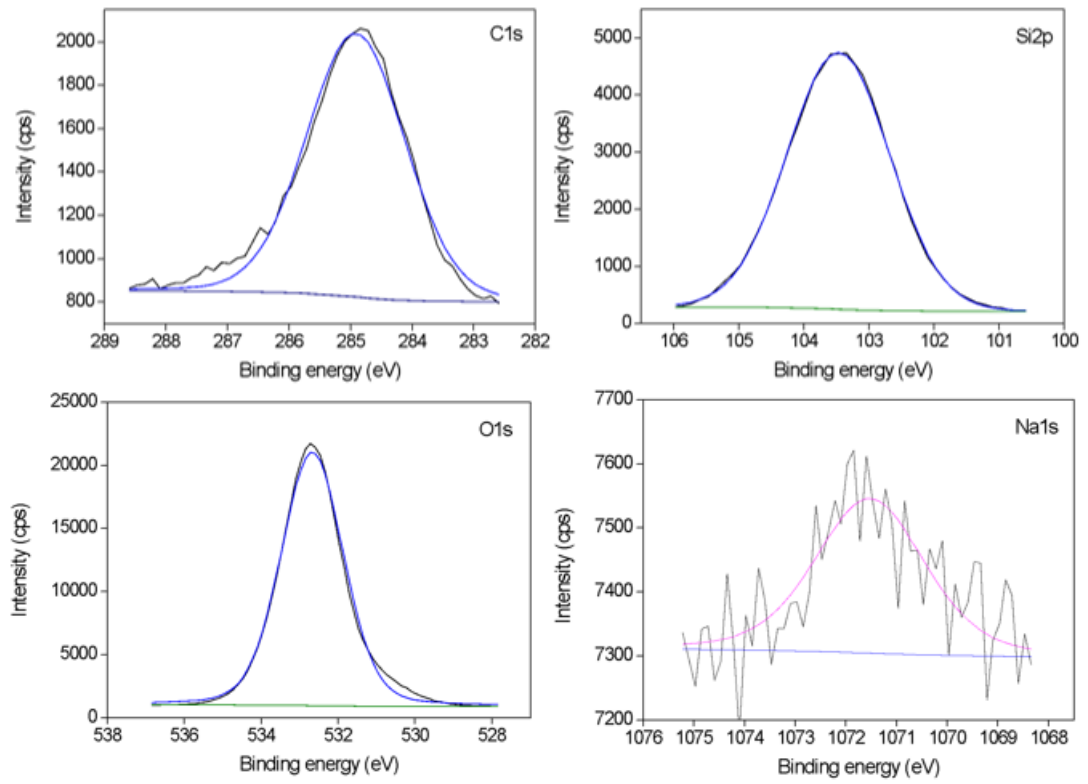
Figure 5.8. XPS decomposed atom electron high-resolution spectra for RH silica.
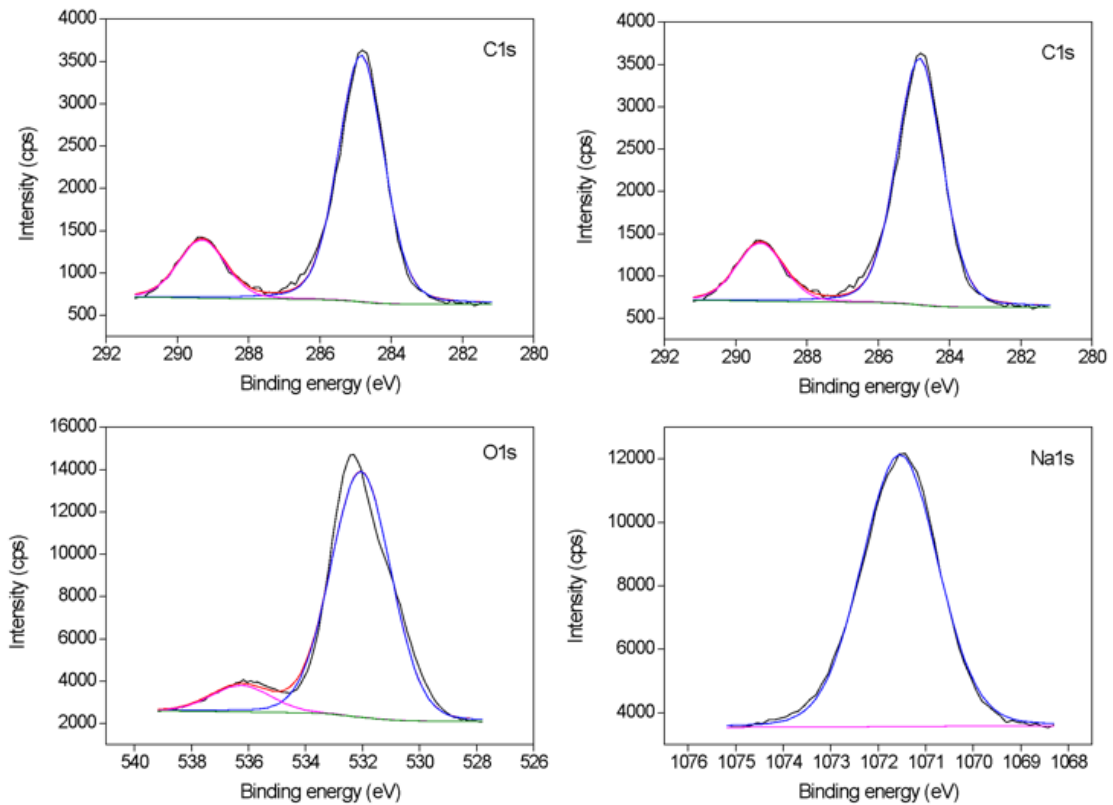
Figure 5.9. XPS decomposed atom electron high-resolution spectra for SG silica.

In all the spectra of O1s (Figures 6.7, 6.8, and 6.9) it is possible to verify that the total oxygen of the surface of the nanomaterials is related to the siloxane group Si−O−Si (~532-533 eV) (Montes et al., 2020). Total surface oxygen follows the order CS > SG > RH (Table 6.4). These amounts are related to different synthesis processes that can lead to different degrees of water chemisorption on the surface of nanoparticles, which is closely related to the presence of oxygen-containing groups on the surfaces.

5.3.2   Characterization of nanofluids

To quantify the stability of nanofluids their zeta-potential was measured after different standing times, as shown in Table 6.5. High zeta potential values indicate that the particles are electrically stable due to electrostatic repulsion (Agi et al., 2020). The repulsive and attractive forces determine the stability of suspensions when solid particles collide with each other in a

liquid medium (Chaturvedi and Chamra, 2021; Khoramian et al, 2022). According to Setia et al. (2013), a nanofluid exhibiting a value of zeta potential greater than 30 mV and lower than -30 mV is stable and resists agglomeration. As shown in Table 6.5, CS-NF0.10 and SG-NF0.10 are stable, while RH-NF0.10 has limited stability (Müller, 1996).

Table 5.5. Average of the nanofluids particle size and zeta potential (ZP) after different standing times.
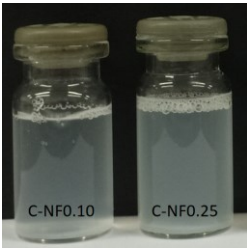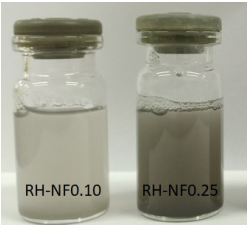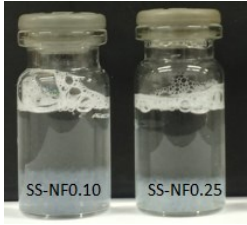
Samples	1st day		30th day	
	Size (nm)	ZP (mV)	Size (nm)	ZP (mV)
CS-NF0.10	3772	-31.1	1331	-34.9
RH-NF0.10	1370	-25.8	3939	-19.5
SG-NF0.10	1863	-19.2	1082	-41.7

The RH-nanoparticles tend to agglomerate over time (Table 6.5) because of inter-particle adhesion The RH-nanoparticles tend to agglomerate over time (Table 6.5) because of inter-particle adhesion forces. The average size of the silica nanoparticles in RH-NF0.10 grew visibly in the nanofluids (Tables 6.5 and 6.6). The main reason for this change may be the aggregation of the nanoparticles, which can be confirmed by the observed change in the zeta potential values (Khoramian et al., 2022). On the other hand, SG-nanoparticles remain non-agglomerated and well-dispersed in the nanofluid (Zulfiqar et al., 2016).

forces. The average size of the silica nanoparticles in RH-NF0.10 grew visibly in the nanofluids (Tables 6.5 and 6.6). The main reason for this change may be the aggregation of the nanoparticles, which can be confirmed by the observed change in the zeta potential values (Khoramian et al., 2022). On the other hand, SG-nanoparticles remain non-agglomerated and well-dispersed in the nanofluid (Zulfiqar et al., 2016).

The stability of nanofluids was also evaluated by measuring their turbidity after different standing times of dispersion after sonication (Table 6.6). This technique is useful for nanoparticle stability studies and can reveal nanoparticle agglomeration and sedimentation as well as quantify nanoparticle stability. As expected, Table 6.6 shows that the increase in the solid content leads to an increase in the light backscattering. On increasing the solid content, the agglomerate size increases, and the turbidity is also increased, but remains nearly constant after 24 h and indicates the stability of nanofluids (Yousefvand et al., 2018).

Table 5.6. Turbidity of the nanofluids after different standing times (left) and images (right).

Nanofluid	Turbidity (NTU)			Images of NF after 24 h of sonication
	Standing time of dispersion after sonication			
	0 h	1 h	24 h	
C-NF0.10	167	181	165	
C-NF0.25	291	344	310	
RH-NF0.10	167	169	139	
RH-NF0.25	169	172	161	
SG- NF0.10	8.8	5.2	55	
SG- NF0.25	25.0	15.3	88	

To achieve high oil recovery, it has been proposed that the nanofluid viscosity should be of the same order of magnitude as the viscosity of the oil. When the viscosity of the nanofluid is much smaller than the viscosity of the oil, the nanofluid flow more easily between the pores in the direction of the production pools, without removing the oil of the pores, resulting in a low recovery factor (Javornik, 2013). It is known that the viscosity of nanofluid can be altered by altering concentration, particle size, and shape, hydrophobic-hydrophilic character, presenting Newtonian or non-Newtonian behavior, etc.

In the present study, the viscosity at different concentrations of silica nanoparticles showed that shear stress increases linearly with an increase in shear rate, indicating Newtonian behavior for the nanofluids. The size of the particle has a direct relationship with the viscosity of the nanofluids (Khoramian, et al., 2022; Maheshwary et al., 2017), and large particles usually form highly viscous nanofluids (Mishra et al., 2014). Although the nanoparticles are agglomerated in CS and RH-nanofluids, the nanofluid viscosity decreases in the order SG-NF > RH-NF to CS-NF, which follows a similar order of nanoparticle sizes (SG >> RH > CS). Moreover, Table 6.7 shows a tendency to increase the viscosity for all nanofluids with the nanoparticle concentration, even at a low concentration (Mishra et al., 2014).

Table 5.7. Viscosity and surface tension of the solutions.

	Viscosity (mPa·s)	Interfacial tension (mN·m^{-1})
Oil	473.13	22.4 ± 0.2
Water	1.37	70.9 ± 0.6
B	0.73	66.9 ± 0.5
BS	0.75	37.3 ± 0.05
CS-NF0.10	0.60	29.2 ± 0.01
CS-NF0.25	0.68	29.5 ± 0.07
CS-NF0.50	0.89	26.6 ± 0.14
CS-NF0.75	0.81	28.4 ± 0.13
RH-NF0.10	0.77	28.1 ±0.03
RH-NF0.25	0.69	30.4 ± 0.01
RH-NF0.50	0.81	30.1 ± 0.02
RH-NF0.75	0.63	30.2 ± 0.03
SG-NF0.50	1.10	27.5 ± 0.01
SG-NF0.75	1.70	26.7 ± 0.13

* The SG-NF0.10 and SG-NF0.25 samples were not measured

The interfacial tension of the oil and the injected nanofluid is one of the main characteristics to determine the movement and the distribution of the fluids in porous media (Sá

et al., 2018; Ali et al., 2020a). As shown in Table 6.7, the interfacial tension is nearly independent of the nanoparticle concentration for CS and SG-nanofluids and increases with the nanoparticle concentration for RH-nanofluid. Comparing characteristics of the nanoparticles with the nanofluids, looking at the surface tension, it seems that the textural properties do not show relevance, indicating that the surface composition is most important, indicating that the surfactant is heard chemically.

5.3.3 Flooding tests

Table 6.8 shows the oil recovery from each step of the oil recovery using different nanofluids. Tests with solutions B and BS were also conducted to evaluate the effect of salt and surfactant on oil removal, respectively. After oil recovery in the first and secondary oil recovery, around 58% of the oil is recovered.

Table 5.8. Oil recovery after flooding tests using B, BS, and different nanofluids

Solution	Recovery Factor (%)		
B	47.8 ± 5.9		
BS	10.1 ± 1.5		
Nanofluids	**CS-NF**	**RH-NF**	**SG-NF**
NF0.10	4.7	4.7	6.8
NF0.25	5.3	8.9	7.4
NF0.50	5.8	5.8	10.0
NF0.75	7.9	5.8	7.9

The nanofluid enhanced oil recovery in this study is higher than that reported by Chaturvedi and Charma (2021) with nanofluids containing 0.10 to 0.75 wt% silica nanoparticles, using oil from the Tarapur Oilfield. On the other hand, 13.37% to 20.87% of oil recovery was reached by Yousefvand et al. (2018) in nanofluid enhanced oil recovery using HPAM as an additive in their silica-based nanofluid to recover heavy oil.

In general, the tertiary oil recovery using CS-NF increases as the nanoparticle

concentration increases, due to the increase in the viscosity, as also reported by Lashari and Ganat (2020). No significant effect of the interfacial tension was observed for all nanofluids. The crystallinity also do not show a significant effect in the oi recovery, considering the similar amount of oil recovered with the CS and RH samples. Additionally, CS-NF and RH-NF result in similar recovery factors, indicating that rice husk ash is a promisor material to produce nanofluids, environmental friendly. It is known that the increment of NPs concentration could reduce the reservoir fluids' IFT, accompanied by a substantial change in wettability on rock surfaces, the repulsive forces between nanoparticles increase the viscosity of the nanofluids (Kumar et al., 2022), which contributes to the enhancement of displacement efficiency (Table 6.8).

CS and RH nanoparticles do not seem retained in the sand bed since the nanofluid turbidity showed a slight increase after the flooding test (Mansouri et al., 2019). However, SG nanoparticles are retained in the sand bed, causing a decrease in the SG-NF0.10 and SG-NF0.25 turbidity, as shown in Figure 6.10, which becomes more important as the nanoparticle concentration increases, what may cause the reduction of oil recovery.
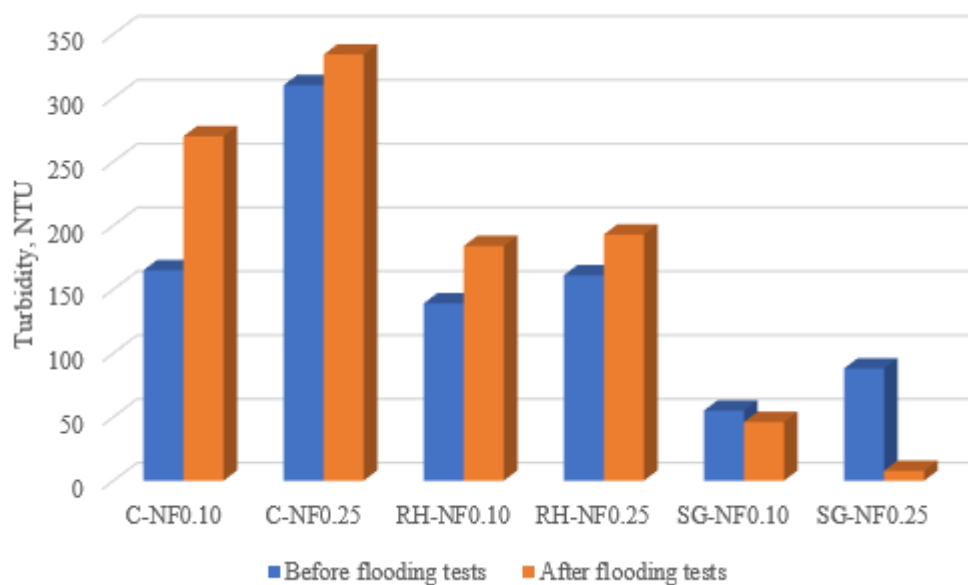
Figure 5.10. Turbidity of different nanofluids before and after flooding tests.

Thus, increasing the SG nanoparticles concentration could decrease the permeability of reservoir rock with high clogging coefficients (Abiz et al., 2021).

5.4   CONCLUSIONS

The current study was an experimental investigation of various sources of silica nanoparticles to produce nanofluids applicable in enhanced oil recovery (EOR). Rice husk ash proved to be a suitable raw material to produce crystalline and nanosized material useful in EOR. With nanoparticles concentration in the range of 0.10 to 0.75 wt%, stable nanofluids were prepared using rice husk ash silica and sol-gel silica with viscosity and interfacial tension similar to the nanofluids formulated using commercial nano silica. Although the nanoparticles can be agglomerated after 24 h-standing times, the stability of nanofluids is guaranteed by a suitable repulsive force and zeta potential more negative than -30 mV. So, in this experimental conditions, an additional 5-10% oil recovery is achieved after flooding due to the injection of nanofluids, proving that silica from rice husk ash has comparable efficiency to other synthetic silica nanoparticles for application in enhanced oil recovery.

6 FINAL REMARKS

The review about the application of nanoparticles in EOR points out that the choice of the nanoparticle must be accordingly several factors for the optimization of the nanofluid. The viscosity of nanofluid must be close to that of oil to achieve higher recovery factors, with viscosity being particularly dependent on the type and concentration of the surfactant and not modified by the size of the nanoparticle. The apparent characteristics of the nanofluid, like viscosity, surface tension, wettability, and contact angle depend on the interaction and adsorption of surfactant and nanoparticle. And the size of the nanoparticle, which must be nanometric, does not interfere much with the recovery factor in enhanced oil recovery processes using nanofluids. In addition, foam stabilization by adjusting the size of the nanoparticles does not have a direct influence on the recovery factor. The nanofluid interfacial tension must be below, although there is no consensus on this matter. Finally, about the wettability and contact angle, several studies report that the smallest contact angles do not result in a high recovery factor.

A review of the synthesis of nanoparticles made clear that the application of nanoparticles for enhanced oil recovery has attracted strong research interest and contributed to many experimental investigations. With this review, we can see that nanoparticles produced by different synthesis methods were explored in terms of size, stability, superficial tension, contact angle, and enhanced oil recovery measurements. The injection of nanofluids in rocky reservoirs has shown great ability to change superficial tension and contact angle, which strongly influences the efficiency of oil recovery. Overall, all nanoparticles showed an improvement in oil recovery, but their applications are mainly limited to laboratory scale, and it requires further research to prove their potential for field-scale implementation

Finally, this study also showed an experimental investigation of different kinds of silica nanoparticles, synthesized from rice husk ash, precipitated from sodium silicate, and commercial, with sodium dodecyl sulfate solution, in brine, for enhanced oil recovery in a fixed bed reactor system simulating a reservoir. The analyzed characteristics like, viscosity, surface tension, and turbidity do not show a direct and significant relationship with the recoveries factor. The best recovery was obtained with the precipitated silica from sodium silicate in a concentration of 0.5 wt%, which recovered 10% of the oil. And the second-best recovery was

obtained by injecting the synthesized silica from rice husk ash, with a concentration of 0.25 wt%, which had a recovery factor of 8.95%.

7 SUGGESTIONS FOR FUTURE WORK

- Carry out the test using crude oil with the same experimental system;

- Perform the same procedure using sea water;

- Improve the method of obtaining silica through sodium silicate, to obtain a purer material;

- Test silica obtained through other synthesis methods;

- Perform the tests using a transparent reservoir to observe the fluid dynamics;

- Use different types of nanoparticles, such as metallic or biological materials;

- Test the same procedure with different concentrations of surfactant;

- Perform recovery test at lower flood speed.

8 REFERENCES

Abang, G. N., Pin, Y. S., Ridzuan, N. (2021). Application of silica (SiO_2) nanofluid and Gemini surfactants to improve the viscous behavior and surface tension of water-based drilling fluids, *Egyptian Journal of Petroleum*, 30(4), 37-42. https://doi.org/10.1016/j.ejpe.2021.10.002

Abiz, M. R., Norouzi-Apourvari, S., Jafari, S., Schaffie, M. (2021). The effect of subsurface factors on the performance of nanofluid-assisted enhanced oil recovery: Modeling and sensitivity analysis, *Journal of Petroleum Science and Engineering*, 202, 108553.

Adil, M., Mohd Zaid, H., & Kean Chuan, L. (2020). Electromagnetically-induced change in interfacial tension and contact angle of oil droplet using dielectric nanofluids. *Fuel*, *259*, 116274. https://doi.org/10.1016/j.fuel.2019.116274

AfzaliTabar, M., Rashidi, A., Alaei, M., Koolivand, H., Pourhashem, S., & Askari, S. (2020). Hybrid of quantum dots for interfacial tension reduction and reservoir alteration wettability for enhanced oil recovery (EOR). *Journal of Molecular Liquids*, *307*, 112984. https://doi.org/10.1016/j.molliq.2020.112984

Agi, A., Junin, R., Jaafar, M. Z., Mohsin, R., Arsad, A., Gbadamosi, A., Fung, C. K., & Gbonhinbor, J. (2020). Synthesis and application of rice husk silica nanoparticles for chemical enhanced oil recovery. *Journal of Materials Research and Technology*, *9* (6), 13054–13066. https://doi.org/10.1016/j.jmrt.2020.08.112

AfzaliTabar, M., Rashidi, A., Alaei, M., Koolivand, H., Pourhashem, S., & Askari, S. (2020). Hybrid of quantum dots for interfacial tension reduction and reservoir alteration wettability for enhanced oil recovery (EOR). *Journal of Molecular Liquids*, *307*, 112984. https://doi.org/10.1016/j.molliq.2020.112984

Ali, H., Soleimani, H., Yahya, N., Khodapanah, L., Sabet, M., Demiral, B. M. R., Hussain, T., Adebayo, L. L. (2020). Enhanced oil recovery by using electromagnetic-assisted nanofluids: A review. *Journal of Molecular Liquids,* 309, 113095. https://doi.org/10.1016/j.molliq.2020.113095

Ali, J. A., Kalhury, A. M., Sabir, A. N., Ahmed, R. N., Ali, N. H., & Abdullah, A. D. (2020a). A state-of-the-art review of the application of nanotechnology in the oil and gas industry with a focus on drilling engineering. *Journal of Petroleum Science and Engineering*, *191*, 107118. https://doi.org/10.1016/j.petrol.2020.107118

Ali, J. A., Kolo, K., Manshad, A. K., Mohammadi, A. H. (2018) Recent advances in

application of nanotechnology in chemical enhanced oil recovery: Effects of nanoparticles on wettability alteration, interfacial tension reduction, and flooding, *Egyptian Journal of Petroleum*, 27 (4) 1371-1383. https://doi.org/10.1016/j.ejpe.2018.09.006

Ali, J. A., Kolo, K., Manshad, A. K., & Stephen, K. D. (2019). Potential application of low-salinity polymeric-nanofluid in carbonate oil reservoirs: IFT reduction, wettability alteration, rheology and emulsification characteristics. *Journal of Molecular Liquids*, *284*, 735–747. https://doi.org/10.1016/j.molliq.2019.04.053

Alomair, O. A., Matar, K. M., & Alsaeed, Y. H. (2015). Experimental Study of Enhanced-Heavy-Oil Recovery in Berea Sandstone Cores by Use of Nanofluids Applications. *SPE Reservoir Evaluation & Engineering*, *18*(03), 387–399. https://doi.org/10.2118/171539-PA

Arunmetha, S., Karthik, A., Srither, S. R., Vinoth, M., Suriyaprabha, R., Manivasakan, P., & Rajendran, V. (2015). Size-dependent physicochemical properties of mesoporous nanosilica produced from natural quartz sand using three different methods. *RSC Advances*, *5*(59), 47390–47397. https://doi.org/10.1039/c5ra07074k

Asl, H. F., Zargar, G., Manshad, A. K., Takassi, M. A., Ali, J. A., & Keshavarz, A. (2020). Effect of SiO2 nanoparticles on the performance of L-Arg and L-Cys surfactants for enhanced oil recovery in carbonate porous media. *Journal of Molecular Liquids*, *300*, 112290. https://doi.org/10.1016/j.molliq.2019.112290

Athinarayanan, J., Periasamy, V. S., Alhazmi, M., Alatiah, K. A., & Alshatwi, A. A. (2015). Synthesis of biogenic silica nanoparticles from rice husks for biomedical applications. *Ceramics International*, *41*(1), 275–281. https://doi.org/10.1016/j.ceramint.2014.08.069

Azevedo, B.R.S.; Gramatges, A.P. (2016). Estabilidade De Espumas Líquidas De Soluções De Surfactantes : Efeito De Misturas E Adição De Nanopartículas. *Revista Brasileira de Iniciação Científica. 3*(7), 54–63.

Awais, M., Bhuiyan, A. A., Salehin, S., Ehsan, M. M., Khan B., Rahman, M. H. (2021). Synthesis, heat transport mechanisms and thermophysical properties of nanofluids: A critical overview, *International Journal of Thermofluids,* 10, 100086.https://doi.org/10.1016/j.ijft.2021.100086

Bakdash, R. S., Aljundi, I. H., Basheer, C., & Abdulazeez, I. (2020). Rice husk derived Aminated Silica for the efficient adsorption of different gases. *Scientific Reports*, *10* (1), 19526. https://doi.org/10.1038/s41598-020-76460-0

Baragau, I. A., Lu, Z., Power, N. P., Morgan, D. J., Bowen, J., Diaz, P., & Kellici, S. (2021). Continuous hydrothermal flow synthesis of S-functionalised carbon quantum dots for

enhanced oil recovery. *Chemical Engineering Journal*, *405*(July 2020), 126631. https://doi.org/10.1016/j.cej.2020.126631

Behera, U. S., Sangwai, J. S. (2022). Silica nanofluid in low salinity seawater containing surfactant and polymer: Oil recovery efficiency, wettability alteration and adsorption studies, *Journal of Petroleum Science and Engineering*, 211,110148.https://doi.org/10.1016/j.petrol.2022.110148

Betancur, S., Olmos, C. M., Pérez, M., Lerner, B., Franco, C. A., Riazi, M., Gallego, J., Carrasco-Marín, F., & Cortés, F. B. (2020). A microfluidic study to investigate the effect of magnetic iron core-carbon shell nanoparticles on displacement mechanisms of crude oil for chemical enhanced oil recovery. *Journal of Petroleum Science and Engineering*, *184*, 106589. https://doi.org/10.1016/j.petrol.2019.106589

Campelo, P. H., Sant'Ana, A. S., & Pedrosa Silva Clerici, M. T. (2020). Starch nanoparticles: production methods, structure, and properties for food applications. *Current Opinion in Food Science*, *33*, 136–140. https://doi.org/10.1016/j.cofs.2020.04.007

Chaturvedi, K. R., Sharma, T. (2021). Rheological analysis and EOR potential of surfactant treated single-step silica nanofluid at high temperature and salinity. *Journal of Petroleum Science and Engineering*, *196*, 107704. https://doi.org/10.1016/j.petrol.2020.107704

Chen, Q., Jiang, X., & Zhen, J. (2021). Preparation and characterization of temperature sensitive iron oxide nanoparticle and its application on enhanced oil recovery. *Journal of Petroleum Science and Engineering*, *198*, 108211. https://doi.org/10.1016/j.petrol.2020.108211

Cheraghian, G., Kiani, S., Nassar, N. N., Alexander, S., & Barron, A. R. (2017). Silica Nanoparticle Enhancement in the Efficiency of Surfactant Flooding of Heavy Oil in a Glass Micromodel. *Industrial & Engineering Chemistry Research*, *56*(30), 8528–8534. https://doi.org/10.1021/acs.iecr.7b01675

Curbelo, F. D. D. S. (2006). Recuperação Avançada De Petróleo Utilizando Tensoativos. 190 f. Thesis (Doctor). Graduation in Chemical Engineering. Federal University of Rio Grande do Norte, Natal, RN.

Daltin, D. (2011). *Tensoativos: química, propriedades e aplicações* (1st ed.). Blucher.

Davydov, V., Rakhmanina, A., Kireev, I., Alieva, I., Zhironkina, O., Strelkova, O., Dianova, V., Samani, T. D., Mireles, K., Yahia, H., Uzbekov, R., Agafonov, V., & Khabashesku, V. (2014). *Solid state synthesis of carbon-encapsulated iron carbide nanoparticles and their interaction with living cells*. https://doi.org/10.1039/c3ta21599g

Divandari, H., Hemmati-Sarapardeh, A., Schaffie, M., & Ranjbar, M. (2019). Integrating synthesized citric acid-coated magnetite nanoparticles with magnetic fields for enhanced oil recovery: Experimental study and mechanistic understanding. *Journal of Petroleum Science and Engineering*, *174*, 425–436. https://doi.org/10.1016/j.petrol.2018.11.037

Dolgov, A., Lopaev, D., Lee, C. J., Zoethout, E., Medvedev, V., Yakushev, O., & Bijkerk, F. (2015). Characterization of carbon contamination under ion and hot atom bombardment in a tin-plasma extreme ultraviolet light source. *Applied Surface Science*, *353*, 708–713. https://doi.org/10.1016/j.apsusc.2015.06.079

Dong, X., Liu, H., Chen, Z., Wu, K., Lu, N., & Zhang, Q. (2019). Enhanced oil recovery techniques for heavy oil and oilsands reservoirs after steam injection. *Applied Energy*, *239*, 1190–1211. https://doi.org/10.1016/j.apenergy.2019.01.244

Druetta, P., Raffa, P., & Picchioni, F. (2019). Chemical enhanced oil recovery and the role of chemical product design. *Applied Energy*, *252*, 113480. https://doi.org/10.1016/j.apenergy.2019.113480

El-hoshoudy, A. N., Desouky, S. E. M., Elkady, M. Y., Al-Sabagh, A. M., Betiha, M. A., & Mahmoud, S. (2017). Hydrophobically associated polymers for wettability alteration and enhanced oil recovery – Article review. *Egyptian Journal of Petroleum*, *26*(3), 757–762. https://doi.org/10.1016/j.ejpe.2016.10.008

Eltoum, H., Yang, Y.-L., & Hou, J.-R. (2021). The effect of nanoparticles on reservoir wettability alteration: a critical review. *Petroleum Science*, *18*(1), 136–153. https://doi.org/10.1007/s12182-020-00496-0

Esene, C., Rezaei, N., Aborig, A., & Zendehboudi, S. (2019). Comprehensive review of carbonated water injection for enhanced oil recovery. *Fuel*, *237*, 1086–1107. https://doi.org/10.1016/j.fuel.2018.08.106

Faghri, A., & Zhang, Y. (2006). Solid-Liquid-Vapor Phenomena and Interfacial Heat and Mass Transfer. In *Transport Phenomena in Multiphase Systems* (pp. 331–420). Elsevier. https://doi.org/10.1016/B978-0-12-370610-2.50010-6

Foroozesh, J., & Kumar, S. (2020). Nanoparticles behaviors in porous media: Application to enhanced oil recovery. *Journal of Molecular Liquids*, *316*, 113876. https://doi.org/10.1016/j.molliq.2020.113876

Franco-Aguirre, M., Zabala, R. D., Lopera, S. H., Franco, C. A., & Cortés, F. B. (2018). Interaction of anionic surfactant-nanoparticles for gas - Wettability alteration of sandstone in

tight gas-condensate reservoirs. *Journal of Natural Gas Science and Engineering*, *51*, 53–64. https://doi.org/10.1016/j.jngse.2017.12.027

Gbadamosi, A. O., Junin, R., Manan, M. A., Yekeen, N., Agi, A., & Oseh, J. O. (2018). Recent advances and prospects in polymeric nanofluids application for enhanced oil recovery. *Journal of Industrial and Engineering Chemistry*, *66*, 1–19. https://doi.org/10.1016/j.jiec.2018.05.020

Giraldo, L. J., Gallego, J., Villegas, J. P., Franco, C. A., & Cortés, F. B. (2019). Enhanced waterflooding with NiO/SiO2 0-D Janus nanoparticles at low concentration. *Journal of Petroleum Science and Engineering*, *174*(June 2018), 40–48. https://doi.org/10.1016/j.petrol.2018.11.007

Guerrero, M., Ruiz, M. P., Millera, Á., Alzueta, M. U., Bilbao, R. (2008). Characterization of biomass chars formed under different devolatilization conditions: differences between rice husk and eucalyptus, *Energy Fuel*s, 22, 1275-1284. https://doi.org/10.1021/ef7005589

Hou, J., Du, J., Sui, H., & Sun, L. (2022). A review on the application of nanofluids in enhanced oil recovery. *Frontiers of Chemical Science and Engineering*. https://doi.org/10.1007/s11705-021-2120-4

Idogun, A., K., Iyagba, E. T., Ukwotije-Ikwut, R. P., Aseminaso, A. (2016). A Review Study of Oil Displacement Mechanisms and Challenges of Nanoparticle Enhanced Oil Recovery, Proceedings of SPE Nigeria Annual International Conference and Exhibition, SPE-184352-MS. https://doi.org/10.2118/184352-MS

Izadi, N., Koochi, M. M., Amrollahi, A., & Pourkhalil, M. (2019). Investigation of functionalized polyelectrolyte polymer-coated Fe3O4 nanoparticles stabilized in high salinity brine at high temperatures as an EOR agent. *Journal of Petroleum Science and Engineering*, *178*(September 2018), 1079–1091. https://doi.org/10.1016/j.petrol.2019.01.074

Jalilian, M., Tabzar, A., Ghasemi, V., Mohammadzadeh, O., Pourafshary, P., Rezaei, N., & Zendehboudi, S. (2019). An experimental investigation of nanoemulsion enhanced oil recovery: Use of unconsolidated porous systems. *Fuel*, *251*, 754–762. https://doi.org/10.1016/j.fuel.2019.02.122

Javornik, G. Aplicação de Nanofluidos na Recuperação Avançada de Petróleo. (2013). 144 f. Thesis (Master). Graduation in Chemical Engineering, Federal University of Santa Catarina, Florianópolis, SC.

Jeong, M. S., Lee, J. H., & Lee, K. S. (2019). Critical review on the numerical modeling of in-situ microbial enhanced oil recovery processes. *Biochemical Engineering Journal*, *150*, 107294. https://doi.org/10.1016/j.bej.2019.107294

Jha, N. K., Ivanova, A., Lebedev, M., Barifcani, A., Cheremisin, A., Iglauer, S., Sangwai, J. S., & Sarmadivaleh, M. (2021). Interaction of low salinity surfactant nanofluids with carbonate surfaces and molecular level dynamics at fluid-fluid interface at ScCO2 loading. *Journal of Colloid and Interface Science*, *586*, 315–325. https://doi.org/10.1016/j.jcis.2020.10.095

Jia, H., Dai, J., Miao, L., Wei, X., Tang, H., Huang, P., Jia, H., He, J., Lv, K., & Liu, D. (2021). Potential application of novel amphiphilic Janus-SiO2 nanoparticles stabilized O/W/O emulsion for enhanced oil recovery. *Colloids and Surfaces A: Physicochemical and Engineering Aspects*, *622*(April), 126658. https://doi.org/10.1016/j.colsurfa.2021.126658

Jiang, S., Chen, Q., Tripathy, M., Luijten, E., Schweizer, K. S., & Granick, S. (2010). Janus Particle Synthesis and Assembly. *Advanced Materials*, *22*(10), 1060–1071. https://doi.org/10.1002/adma.200904094

Ju, B., Fan, T., & Li, Z. (2012). Improving water injectivity and enhancing oil recovery by wettability control using nanopowders. *Journal of Petroleum Science and Engineering*, *86–87*, 206–216. https://doi.org/10.1016/j.petrol.2012.03.022

Kang, X., Zhang, J., Sun, F., Zhang, F., Feng, G., Yang, J., Zhang, X., & Xiang, W. (2011, July 19). A Review of Polymer EOR on Offshore Heavy Oil Field in Bohai Bay, China. *All Days*. https://doi.org/10.2118/144932-MS

Keykhosravi, A., Vanani, M. B., Daryasafar, A., & Aghayari, C. (2021). Comparative study of different enhanced oil recovery scenarios by silica nanoparticles: An approach to time-dependent wettability alteration in carbonates. *Journal of Molecular Liquids*, *324*, 115093. https://doi.org/10.1016/j.molliq.2020.115093

Khoramian, R., Kharrat, R., & Golshokooh, S. (2022). The development of novel nanofluid for enhanced oil recovery application. *Fuel*, *311*, 122558. https://doi.org/10.1016/j.fuel.2021.122558

Ko, E. B., & Kim, J.-Y. (2021). Application of starch nanoparticles as a stabilizer for Pickering emulsions: Effect of environmental factors and approach for enhancing its storage stability. *Food Hydrocolloids*, *120*, 106984. https://doi.org/10.1016/j.foodhyd.2021.106984

Kondiparty, K., Nikolov, A., Wu, S., & Wasan, D. (2011). Wetting and Spreading of Nanofluids on Solid Surfaces Driven by the Structural Disjoining Pressure: Statics Analysis and Experiments. *Langmuir*, *27*(7), 3324–3335. https://doi.org/10.1021/la104204b

Kuang, W., Saraji, S., & Piri, M. (2018). A systematic experimental investigation on the synergistic effects of aqueous nanofluids on interfacial properties and their implications for enhanced oil recovery. *Fuel*, *220*(February), 849–870. https://doi.org/10.1016/j.fuel.2018.01.102

Kumar, N., Gaur, T., & Mandal, A. (2017). Characterization of SPN Pickering emulsions for application in enhanced oil recovery. *Journal of Industrial and Engineering Chemistry*, *54*, 304–315. https://doi.org/10.1016/j.jiec.2017.06.005

Kumar, D., Lashari, N., Ganat, T., Ayoub, M. A., Soomro, A. A., Chandio, T. A. (2022) A review on application of nanoparticles in cEOR: Performance, mechanisms, and influencing parameters, *Journal of Molecular Liquid*s, 353 (1), 118821. https://doi.org/10.1016/j.molliq.2022.118821

Kumar, S., & Mandal, A. (2017). A comprehensive review on chemically enhanced water alternating gas/CO2 (CEWAG) injection for enhanced oil recovery. *Journal of Petroleum Science and Engineering*, *157*, 696–715. https://doi.org/10.1016/j.petrol.2017.07.066

Lashari, N., Ganat, T. (2020) Emerging applications of nanomaterials in chemical enhanced oil recovery: Progress and perspective, Chinese Journal of Chemical Engineering, 28 (8), 1995-2009. https://doi.org/10.1016/j.cjche.2020.05.019

Lau, H. C., Yu, M., & Nguyen, Q. P. (2017). Nanotechnology for oilfield applications: Challenges and impact. *Journal of Petroleum Science and Engineering*, *157*, 1160–1169. https://doi.org/10.1016/j.petrol.2017.07.062

Liu, R., Pu, W., Sheng, J. J., & Du, D. (2017). CO2-switchable nanohybrids for enhancing CO2 flooding in tight reservoirs: From stable colloids to a relevant viscoelastic fluid. *Materials and Design*, *133*, 487–497. https://doi.org/10.1016/j.matdes.2017.08.023

López, D., Zabala, R. D., Cárdenas, J. C., Lopera, S. H., Riazi, M., Franco, C. A., & Cortés, F. B. (2020). A novel design of silica-based completion nanofluids for heavy oil reservoirs. *Journal of Petroleum Science and Engineering*, *194*(June). https://doi.org/10.1016/j.petrol.2020.107483

Maaref, S., Kantzas, A., & Bryant, S. (2020). Investigating sweep efficiency improvement in oil-wet porous media by the application of functionalized nanoparticles. *Fuel*, *267*, 117263. https://doi.org/10.1016/j.fuel.2020.117263

Maheshwary, P. B., Handa, C. C., & Nemade, K. R. (2017). A comprehensive study of effect of concentration, particle size and particle shape on thermal conductivity of titania/water based nanofluid. *Applied Thermal Engineering*, *119*, 79–88. https://doi.org/10.1016/j.applthermaleng.2017.03.054

Mamani, J. B. (2009). 200 f. *Estrutura e propriedades de nanopartículas preparadas via sol-gel*. Thesis (Doctor). Graduation in Science, Federal University of São Paulo, São Paulo, SP. https://doi.org/10.11606/T.43.2009.tde-24082009-090624

Mansouri, M., Nakhaee, A., Pourafshary, P. (2019). Effect of SiO_2 nanoparticles on fines stabilization during low salinity water flooding in sandstones, *Journal of Petroleum Science and Engineering*, 174, 637-648. https://doi.org/10.1016/j.petrol.2018.11.066

Matias, I.A.S. Nanofluidos para aplicações energéticas. (2016) 152f. Thesis (Master). Graduation in Chemical and Biological Engineering. Higher Institute of Engineering of Lisbon, Lisbon.

Maurya, N. K., & Mandal, A. (2016). Studies on behavior of suspension of silica nanoparticle in aqueous polyacrylamide solution for application in enhanced oil recovery. *Petroleum Science and Technology*, *34*(5), 429–436. https://doi.org/10.1080/10916466.2016.1145693

Maurya, N. K., Kushwaha, P., & Mandal, A. (2017). Studies on interfacial and rheological properties of water soluble polymer grafted nanoparticle for application in enhanced oil recovery. *Journal of the Taiwan Institute of Chemical Engineers*, *70*, 319–330. https://doi.org/10.1016/j.jtice.2016.10.021

Mishra, P. C., Mukherjee, S., Nayak, S. K., & Panda, A. (2014). A brief review on viscosity of nanofluids. *International Nano Letters*, *4*(4), 109–120. https://doi.org/10.1007/s40089-014-0126-3

Mittal, A. (2022). Recent advances in using a silica nanofluid for enhanced oil recovery. *Materials Today: Proceedings*, *52*, 1260–1266. https://doi.org/10.1016/j.matpr.2021.11.050

Mohajeri, M., Reza Rasaei, M., & Hekmatzadeh, M. (2019). Experimental study on using SiO2 nanoparticles along with surfactant in an EOR process in micromodel. *Petroleum Research*, *4*(1), 59–70. https://doi.org/10.1016/j.ptlrs.2018.09.001

Montes, D., Henao, J., Taborda, E. A., Gallego, J., Cortés, F. B., & Franco, C. A. (2020). Effect of Textural Properties and Surface Chemical Nature of Silica Nanoparticles from Different Silicon Sources on the Viscosity Reduction of Heavy Crude Oil. *ACS Omega*, *5*(10), 5085–5097. https://doi.org/10.1021/acsomega.9b04041

Müller, R.H., Zetapotential und Partikelladung in der Laborpraxis. 1st ed. 1996, Stuttgart: Wissenschaftliche Verlagsgesellschaft.

Nasr, M. S., Esmaeilnezhad, E., Allahbakhsh, A., & Choi, H. J. (2021). Nitrogen-doped graphene quantum dot nanofluids to improve oil recovery from carbonate and sandstone oil reservoirs. *Journal of Molecular Liquids*, *330*, 115715. https://doi.org/10.1016/j.molliq.2021.115715

Nazarahari, M. J., Manshad, A. K., Ali, M., Ali, J. A., Shafiei, A., Sajadi, S. M., Moradi, S., Iglauer, S., & Keshavarz, A. (2021). Impact of a novel biosynthesized nanocomposite (SiO2@Montmorilant@Xanthan) on wettability shift and interfacial tension: Applications for enhanced oil recovery. *Fuel*, *298*(January), 120773. https://doi.org/10.1016/j.fuel.2021.120773

Negi, G. S., Anirbid, S., & Sivakumar, P. (2021). Applications of silica and titanium dioxide nanoparticles in enhanced oil recovery: Promises and challenges. In *Petroleum Research* 6(3) 224–246. KeAi Publishing Communications Ltd. https://doi.org/10.1016/j.ptlrs.2021.03.001

Negin, C., Ali, S., & Xie, Q. (2016). Application of nanotechnology for enhancing oil recovery – A review. *Petroleum*, *2*(4), 324–333. https://doi.org/10.1016/j.petlm.2016.10.002

Nourafkan, E., Hu, Z., & Wen, D. (2018). Nanoparticle-enabled delivery of surfactants in porous media. *Journal of Colloid and Interface Science*, *519*, 44–57. https://doi.org/10.1016/j.jcis.2018.02.032

Olayiwola, S. O., & Dejam, M. (2019). A comprehensive review on interaction of nanoparticles with low salinity water and surfactant for enhanced oil recovery in sandstone and carbonate reservoirs. *Fuel*, *241*, 1045–1057. https://doi.org/10.1016/j.fuel.2018.12.122

Oliveira, G. A. (2012). 121 f. *Síntese e caracterização de nanofluidos de prata*. Thesis (Master). Graduation in Mechanical Engineering, Federal University of Uberlândia, MG.

Omar, M. F., Aziz, H. A., & Stoll, S. (2014). Stability of ZnO Nanoparticles in Solution. Influence of pH, Dissolution, Aggregation and Disaggregation Effects. *Journal of Colloid Science and Biotechnology*, *3*(1), 75–84. https://doi.org/10.1166/jcsb.2014.1072

Omidi, A., Manshad, A. K., Moradi, S., Ali, J. A., Sajadi, S. M., & Keshavarz, A. (2020). Smart- and nano-hybrid chemical EOR flooding using Fe3O4/eggshell nanocomposites. *Journal of Molecular Liquids*, *316*, 113880. https://doi.org/10.1016/j.molliq.2020.113880

Panahpoori, D., Rezvani, H., Parsaei, R., & Riazi, M. (2019). A pore-scale study on improving CTAB foam stability in heavy crude oil−water system using TiO2 nanoparticles.

Journal of Petroleum Science and Engineering, *183*, 106411.
https://doi.org/10.1016/j.petrol.2019.106411

Pereira, M. L. de O., Maia, K. C. B., Silva, W. C., Leite, A. C., Francisco, A. D. dos S., Vasconcelos, T. L., Nascimento, R. S. V., & Grasseschi, D. (2020). Fe 3 O 4 Nanoparticles as Surfactant Carriers for Enhanced Oil Recovery and Scale Prevention. *ACS Applied Nano Materials*, *3*(6), 5762–5772. https://doi.org/10.1021/acsanm.0c00939

Radnia, H., Rashidi, A., Solaimany Nazar, A. R., Eskandari, M. M., & Jalilian, M. (2018). A novel nanofluid based on sulfonated graphene for enhanced oil recovery. *Journal of Molecular Liquids*, *271*, 795–806. https://doi.org/10.1016/j.molliq.2018.09.070

Rahman, I. A., & Padavettan, V. (2012). Synthesis of Silica nanoparticles by Sol-Gel: Size-dependent properties, surface modification, and applications in silica-polymer nanocompositesa review. *Journal of Nanomaterials*, *2012*(May). https://doi.org/10.1155/2012/132424

Raj, I., Qu, M., Xiao, L., Hou, J., Li, Y., Liang, T., Yang, T., & Zhao, M. (2019). Ultralow concentration of molybdenum disulfide nanosheets for enhanced oil recovery. *Fuel*, *251*, 514–522. https://doi.org/10.1016/j.fuel.2019.04.078

Rangel, I. R., Thompson, R. L., Pereira, R. G., & Abreu, F. L. B. de. (2012). Experimental investigation of the enhanced oil recovery process using a polymeric solution. *Journal of the Brazilian Society of Mechanical Sciences and Engineering*, *34*(3), 285–293. https://doi.org/10.1590/S1678-58782012000300009

Rashidi, M., Kalantariasl, A., Saboori, R., Haghani, A., & Keshavarz, A. (2021). Performance of environmental friendly water-based calcium carbonate nanofluid as enhanced recovery agent for sandstone oil reservoirs. *Journal of Petroleum Science and Engineering*, *196*(July 2020), 107644. https://doi.org/10.1016/j.petrol.2020.107644

Rezk, M. Y., & Allam, N. K. (2019). Impact of Nanotechnology on Enhanced Oil Recovery: A Mini-Review. *Industrial & Engineering Chemistry Research*, *58*(36), 16287–16295. https://doi.org/10.1021/acs.iecr.9b03693

Rezk, M. Y., & Allam, N. K. (2019). Unveiling the Synergistic Effect of ZnO Nanoparticles and Surfactant Colloids for Enhanced Oil Recovery. *Colloids and Interface Science Communications*, *29*(January), 33–39. https://doi.org/10.1016/j.colcom.2019.01.004

Rezvani, H., Panahpoori, D., Riazi, M., Parsaei, R., Tabaei, M., & Cortés, F. B. (2020). A novel foam formulation by Al2O3/SiO2 nanoparticles for EOR applications: A mechanistic

study. *Journal of Molecular Liquids*, *304*, 16–18.
https://doi.org/10.1016/j.molliq.2020.112730

Rognmo, A. U., Heldal, S., & Fernø, M. A. (2018). Silica nanoparticles to stabilize CO2-foam for improved CO2 utilization: Enhanced CO2 storage and oil recovery from mature oil reservoirs. *Fuel*, *216*, 621–626. https://doi.org/10.1016/j.fuel.2017.11.144

Sá, A. B. G. T. de, Serruya, B. S. M., Ferreira, G. de S. (2018). Uso de Nanopartículas na Recuperação de Petróleo. In *III National Congress of Petroleum, Natural Gas, and Biofuel, and V Workshop of Petroleum Engineering - CONEPETRO* (Vol. 1, pp. 1–8). Realize.

Said, Z., Sundar, L. S., Tiwari, A. K., Ali, H. M., Sheikholeslami, M., Bellos, E., & Babar, H. (2022). Recent advances on the fundamental physical phenomena behind stability, dynamic motion, thermophysical properties, heat transport, applications, and challenges of nanofluids. *Physics Reports*, 946, 1–94. https://doi.org/10.1016/j.physrep.2021.07.002

Safdel, M., Anbaz, M. A., Daryasafar, A., & Jamialahmadi, M. (2017). Microbial enhanced oil recovery, a critical review on worldwide implemented field trials in different countries. *Renewable and Sustainable Energy Reviews*, *74*, 159–172.
https://doi.org/10.1016/j.rser.2017.02.045

Saravanan, A., Kumar, P. S., Vardhan, K. H., Jeevanantham, S., Karishma, S. B., Yaashikaa, P. R., & Vellaichamy, P. (2020). A review on systematic approach for microbial enhanced oil recovery technologies: Opportunities and challenges. *Journal of Cleaner Production*, *258*, 120777. https://doi.org/10.1016/j.jclepro.2020.120777

Schneider, M., José, H.J.; Moreira, R.F.P.M. (2021). Aplicação de Nanofluidos na Recuperação Avançada de Petróleo – uma revisão. *Revista Química, Ciência, Tecnologia e Sociedade*, 6 (1).

Setia, H., Gupta, R., Wanchoo, R. K. (2013). Stability of nanofluids, *Materials Science Forum*, 757, 139-149, https://doi.org/10.4028/www.scientific.net/MSF.757.139

Shalbafan, M., Esmaeilzadeh, F., Safaei, A., & XiaopoWang. (2019). Experimental investigation of wettability alteration and oil recovery enhance in carbonate reservoirs using iron oxide nanoparticles coated with EDTA or SLS. *Journal of Petroleum Science and Engineering*, *180*, 559–568. https://doi.org/10.1016/j.petrol.2019.05.085

Shalbafan, M., Esmaeilzadeh, F., Safaei, A., & XiaopoWang. (2019). Experimental investigation of wettability alteration and oil recovery enhance in carbonate reservoirs using iron oxide nanoparticles coated with EDTA or SLS. *Journal of Petroleum Science and Engineering*, *180*(May), 559–568. https://doi.org/10.1016/j.petrol.2019.05.085

Shayan Nasr, M., Esmaeilnezhad, E., Allahbakhsh, A., & Choi, H. J. (2021). Nitrogen-doped graphene quantum dot nanofluids to improve oil recovery from carbonate and sandstone oil reservoirs. *Journal of Molecular Liquids*, *330*, 115715. https://doi.org/10.1016/j.molliq.2021.115715

Shaw, S. (2020). A Review of Nanofluids Synthesis for Oil and Gas Applications. *2020 IEEE 15th International Conference on Nano/Micro Engineered and Molecular System (NEMS)*, 455–460. https://doi.org/10.1109/NEMS50311.2020.9265611

Sircar, A, Rayavarapu, K., Bist, N., Yadav, K., Singh, S. (2022). Applications of nanoparticles in enhanced oil recovery, *Petroleum Research*, 7(1) 77-90.

Soleimani, H., Baig, M. K., Yahya, N., Khodapanah, L., Sabet, M., Demiral, B. M. R., & Burda, M. (2018). Impact of carbon nanotubes based nanofluid on oil recovery efficiency using core flooding. *Results in Physics*, *9*, 39–48. https://doi.org/10.1016/j.rinp.2018.01.072

Son, H., Kim, H., Lee, G., Kim, J., Sung, W. (2014). Enhanced oil recovery using nanoparticle-stabilized oil/water emulsions. *Korean Journal of Chemical Engineering*, *31*(2), 338–342. https://doi.org/10.1007/s11814-013-0214-5

Song, Z., Song, Y., Li, Y., Bai, B., Song, K., & Hou, J. (2020). A critical review of CO2 enhanced oil recovery in tight oil reservoirs of North America and China. *Fuel*, *276*, 118006. https://doi.org/10.1016/j.fuel.2020.118006

Steven, S., Restiawaty, E., Bindar, Y. (2021), Routes for energy and bio-silica production from rice husk: A comprehensive review and emerging prospect, *Renewable and Sustainable Energy Reviews*, 149, 111329, https://doi.org/10.1016/j.rser.2021.111329

Suleimanov, B. A., Ismailov, F. S., Veliyev, E. F. (2011). Nanofluid for enhanced oil recovery. *Journal of Petroleum Science and Engineering*, *78*(2), 431–437. https://doi.org/10.1016/j.petrol.2011.06.014

Sun, Y., Yang, D., Shi, L., Wu, H., Cao, Y., He, Y., & Xie, T. (2020). Properties of Nanofluids and Their Applications in Enhanced Oil Recovery: A Comprehensive Review. *Energy & Fuels*, *34*(2), 1202–1218. https://doi.org/10.1021/acs.energyfuels.9b03501

Taborda, E. A., Franco, C. A., Lopera, S. H., Alvarado, V., & Cortés, F. B. (2016). Effect of nanoparticles/nanofluids on the rheology of heavy crude oil and its mobility on porous media at reservoir conditions. *Fuel*, *184*, 222–232. https://doi.org/10.1016/j.fuel.2016.07.013

Tajik, S., Shahrabadi, A., Rashidi, A., Jalilian, M., & Yadegari, A. (2018). Application of functionalized silica-graphene nanohybrid for the enhanced oil recovery performance.

Colloids and Surfaces A: Physicochemical and Engineering Aspects, *556*(June), 253–265. https://doi.org/10.1016/j.colsurfa.2018.08.029

Tackie-Otoo, B. N., Ayoub Mohammed, M. A., Yekeen, N., & Negash, B. M. (2020). Alternative chemical agents for alkalis, surfactants and polymers for enhanced oil recovery: Research trend and prospects. *Journal of Petroleum Science and Engineering*, *187*, 106828. https://doi.org/10.1016/j.petrol.2019.106828

Taleb, M., Sagala, F., Hethnawi, A., & Nassar, N. N. (2021). Enhanced Oil Recovery from Austin Chalk Carbonate Reservoirs Using Faujasite-Based Nanoparticles Combined with Low-Salinity Water Flooding. *Energy & Fuels*, *35*(1), 213–225. https://doi.org/10.1021/acs.energyfuels.0c02324

Thomas, J.E. (Org.). (2001*). Fundamentos de Engenharia de Petróleo* (2th ed.). Interciência.

Tian, W., Li, H., Zhou, J., & Guo, Y. (2017). Preparation, characterization, and the adsorption characteristics of lignin/silica nanocomposites from cellulosic ethanol residue. *RSC Advances*, *7*(65), 41176–41181. https://doi.org/10.1039/c7ra06322a

Tiwari, A. K., Pandya, N. S., Said, Z., Öztop, H. F., & Abu-Hamdeh, N. (2021). 4S consideration (synthesis, sonication, surfactant, stability) for the thermal conductivity of CeO_2 with MWCNT and water based hybrid nanofluid: An experimental assessment. *Colloids and Surfaces A: Physicochemical and Engineering Aspects*, *610*, 125918. https://doi.org/10.1016/j.colsurfa.2020.125918

U.S. Environmental Protection Agency. (n.d.). *Module 3: Characteristics of Particles, Particle Size Categories*. https://www.epa.gov/

Vert, M., Doi, Y., Hellwich, K.-H., Hess, M., Hodge, P., Kubisa, P., Rinaudo, M., & Schué, F. (2012). Terminology for biorelated polymers and applications (IUPAC Recommendations 2012). *Pure and Applied Chemistry*, *84*(2), 377–410. https://doi.org/10.1351/PAC-REC-10-12-04

Vishnyakov, V., Suleimanov, B., Zeynalov, E., & Salmanov, A. (2020). Oil recovery stages and methods. In *Primer on Enhanced Oil Recovery*, 53–63. Elsevier. https://doi.org/10.1016/C2017-0-03909-5

Viswanathan, B. (2016). *Energy Sources: Fundamentals of Chemical Conversion Processes and Applications* (1st ed.). Elsevier.

Vollath, D., & Szab, D. V. (1999). *<1998 -Szabo-JNanoRes- Coated nanoparticles A new way to improved nanocomposites.pdf>*. 235–242.

Voltatoni, T. (2012). 90 f. Emprego de Ciclodextrinas para recuperação avançada de petróleo. Thesis (Master). Graduation in Energy, Federal University of ABC, Santo André, SP.

Wahaab, F. A., Adebayo, L. L., Adekoya, A. A., Yusuf, J. Y., Obalalu, A. M., Yusuff, A. O., & Alqasem, B. (2020). Electromagnetic wave-induced nanofluid-oil interfacial tension reduction for enhanced oil recovery. *Journal of Molecular Liquids*, *318*, 114378. https://doi.org/10.1016/j.molliq.2020.114378

Wang, X. D., Shen, Z. X., Sang, T., Cheng, X. bin, Li, M. F., Chen, L. Y., & Wang, Z. S. (2010). Preparation of spherical silica particles by Stöber process with high concentration of tetra-ethyl-orthosilicate. *Journal of Colloid and Interface Science*, *341*(1), 23–29. https://doi.org/10.1016/j.jcis.2009.09.018

Wang, X.-D., Shen, Z.-X., Sang, T., Cheng, X.-B., Li, M.-F., Chen, L.-Y., & Wang, Z.-S. (2010). Preparation of spherical silica particles by St?ber process with high concentration of tetra-ethyl-orthosilicate. *Journal of Colloid and Interface Science*, *341*(1), 23–29. https://doi.org/10.1016/j.jcis.2009.09.018

Wang, Z., Fang, R., & Guo, H. (2020). Advances in ultrasonic production units for enhanced oil recovery in China. *Ultrasonics Sonochemistry*, *60*, 104791. https://doi.org/10.1016/j.ultsonch.2019.104791

Wang, Z., Zeng, S., Li, Y., Wang, W., Zhang, Z., Zeng, H., Wang, W., & Sun, L. (2017). Luminescence Mechanism of Carbon-Incorporated Silica Nanoparticles Derived from Rice Husk Biomass. *Industrial and Engineering Chemistry Research*, *56*(20), 5906–5912. https://doi.org/10.1021/acs.iecr.7b00700

Wu, H., Gao, K., Lu, Y., Meng, Z., Gou, C., Li, Z., Yang, M., Qu, M., Liu, T., Hou, J., & Kang, W. (2020). Silica-based amphiphilic Janus nanofluid with improved interfacial properties for enhanced oil recovery. *Colloids and Surfaces A: Physicochemical and Engineering Aspects*, *586*(August 2019), 124162. https://doi.org/10.1016/j.colsurfa.2019.124162

Xu, D., Bai, B., Wu, H., Hou, J., Meng, Z., Sun, R., Li, Z., Lu, Y., & Kang, W. (2019). Mechanisms of imbibition enhanced oil recovery in low permeability reservoirs: Effect of IFT reduction and wettability alteration. *Fuel*, *244*, 110–119. https://doi.org/10.1016/j.fuel.2019.01.118

Yakasai, F., Jaafar, M. Z., Bandyopadhyay, S., & Agi, A. (2021). Current developments and future outlook in nanofluid flooding: A comprehensive review of various parameters influencing oil recovery mechanisms. *Journal of Industrial and Engineering Chemistry*, *93*, 138–162. https://doi.org/10.1016/j.jiec.2020.10.017

Yin, T., Yang, Z., Dong, Z., Lin, M., & Zhang, J. (2019). Physicochemical properties and potential applications of silica-based amphiphilic Janus nanosheets for enhanced oil recovery. *Fuel*, *237*(June 2018), 344–351. https://doi.org/10.1016/j.fuel.2018.10.028

Yuan, B., & Wood, D. A. (2018). A comprehensive review of formation damage during enhanced oil recovery. *Journal of Petroleum Science and Engineering*, *167*, 287–299. https://doi.org/10.1016/j.petrol.2018.04.018

Yousefvand, H. A., & Jafari, A. (2018). Stability and flooding analysis of nanosilica/ NaCl /HPAM/SDS solution for enhanced heavy oil recovery. *Journal of Petroleum Science and Engineering*, *162*, 283–291. https://doi.org/10.1016/j.petrol.2017.09.078

Zainon, S. N. M., & Azmi, W. H. (2021). Stability and thermo-physical properties of green bio-glycol based TiO2-SiO2 nanofluids. *International Communications in Heat and Mass Transfer*, *126*(June). https://doi.org/10.1016/j.icheatmasstransfer.2021.105402

Zamani, H., Jafari, A., Mousavi, S. M., & Darezereshki, E. (2020). Biosynthesis of silica nanoparticles using Saccharomyces cervisiae and its application on enhanced oil recovery. *Journal of Petroleum Science and Engineering*, 190, 107002. https://doi.org/10.1016/j.petrol.2020.107002

Zargar, G., Arabpour, T., Khaksar Manshad, A., Ali, J. A., Mohammad Sajadi, S., Keshavarz, A., & Mohammadi, A. H. (2020). Experimental investigation of the effect of green TiO2/Quartz nanocomposite on interfacial tension reduction, wettability alteration, and oil recovery improvement. *Fuel*, *263*(May 2019), 116599. https://doi.org/10.1016/j.fuel.2019.116599

Zhang, Y. C., You, Y., Xin, S., Yin, Y. X., Zhang, J., Wang, P., Zheng, X. sheng, Cao, F. F., & Guo, Y. G. (2016). Rice husk-derived hierarchical silicon/nitrogen-doped carbon/carbon nanotube spheres as low-cost and high-capacity anodes for lithium-ion batteries. *Nano Energy*, *25*, 120–127. https://doi.org/10.1016/j.nanoen.2016.04.043

Zhao, M., Lv, W., Li, Y., Dai, C., Wang, X., Zhou, H., Zou, C., Gao, M., Zhang, Y., & Wu, Y. (2018). Study on the synergy between silica nanoparticles and surfactants for enhanced oil recovery during spontaneous imbibition. *Journal of Molecular Liquids*, *261*, 373–378. https://doi.org/10.1016/j.molliq.2018.04.034

Zhou, Y., Wu, X., Zhong, X., Reagen, S., Zhang, S., Sun, W., Pu, H., & Xiaojun Zhao, J. (2020). Polymer nanoparticles based nano-fluid for enhanced oil recovery at harsh formation conditions. *Fuel*, *267*(January). https://doi.org/10.1016/j.fuel.2020.117251

Zulfiqar, U., Subhani, T., & Wilayat Husain, S. (2016). Synthesis of silica nanoparticles from sodium silicate under alkaline conditions. *Journal of Sol-Gel Science and Technology*, *77*(3), 753–758. https://doi.org/10.1007/s10971-015-3950-7